University of Alberta

A Mathematical Framework for Expressing Multivariate Distributions Useful in Wireless Communications

by

Kasun T. Hemachandra

A thesis submitted to the Faculty of Graduate Studies and Research in partial fulfillment of the requirements for the degree of

Master of Science

in

Communications

Department of Electrical and Computer Engineering

© Kasun T. Hemachandra
Fall 2010
Edmonton, Alberta

Permission is hereby granted to the University of Alberta Libraries to reproduce single copies of this thesis and to lend or sell such copies for private, scholarly or scientific research purposes only. Where the thesis is converted to, or otherwise made available in digital form, the University of Alberta will advise potential users of the thesis of these terms.

The author reserves all other publication and other rights in association with the copyright in the thesis and, except as herein before provided, neither the thesis nor any substantial portion thereof may be printed or otherwise reproduced in any material form whatsoever without the author's prior written permission.

Examining Committee

Dr. Norman C. Beaulieu, Electrical and Computer Engineering

Dr. Chintha Tellambura, Electrical and Computer Engineering

Dr. Byron Schmuland, Mathematical and Statistical Sciences

To my family

Abstract

Multivariate statistics play an important role in performance analysis of wireless communication systems in correlated fading channels. This thesis presents a framework which can be used to derive easily computable mathematical representations for some multivariate statistical distributions, which are derivatives of the Gaussian distribution, and which have a particular correlation structure. The new multivariate distribution representations are given as single integral solutions of familiar mathematical functions which can be evaluated using common mathematical software packages. The new approach can be used to obtain single integral representations for the multivariate probability density function, cumulative distribution function, and joint moments of some widely used statistical distributions in wireless communication theory, under an assumed correlation structure. The remarkable advantage of the new representation is that the computational burden remains at numerical evaluation of a single integral, for a distribution with an arbitrary number of dimensions. The new representations are used to evaluate the performance of diversity combining schemes and multiple input multiple output systems, operating in correlated fading channels. The new framework gives some insights into some long existing open problems in multivariate statistical distributions.

Acknowledgements

First and foremost I extend my sincere gratitude to my supervisor, Dr. Norman C. Beaulieu, for his support and supervision. His expertise, continuous advice, guidance, feedback and encouragement have been a vital component in making this work a success. I consider it as a great privilege to be part of his team at iCORE Wireless Communications Laboratory (*i*WCL).

I also wish to thank the members of my thesis committee, Dr. Chintha Tellambura and Dr. Byron Schmuland, for their valuable comments and feedback in improving the quality of this thesis.

My heartfelt thanks go to the entire team at *i*WCL for creating a professional and supporting environment during my stay at *i*WCL. I greatly appreciate the support, guidance and friendship of all the members of *i*WCL. It has been a great pleasure working with them.

I am extremely grateful my family, all my relatives and my love Ranu for their love, encouragement and support, without which this work would not have been possible.

Finally I would like to thank all the others who helped me in both academic and non-academic endeavors during my stay in Canada and University of Alberta.

Table of Contents

List of Figures

List of Symbols

Symbol	Definition	First Use
$\exp(x)$	Exponential function	3
$I_\nu(\cdot)$	Modified Bessel function of first kind and order ν	3
$\Gamma(\cdot)$	Gamma function	3
$\mathbb{E}[\cdot]$	Expectation of a random variable	3
$\mathcal{N}(\mu, \sigma^2)$	Gaussian distributed with mean μ and variance σ^2	15
$N_c(\mu, \sigma^2)$	Complex Gaussian distributed with mean μ and variance σ^2	15
$\text{Var}(\cdot)$	Variance of a random variable	15
$\lvert X \rvert$	Magnitude of X	15
X^*	complex conjugate of X	15
$f_X(x)$	Probability density function of X	15
$F_X(x)$	Cumulative distribution function of X	15
$Q(a, b)$	1st order Marcum Q-function	19
$Q_m(a, b)$	m^{th} order generalized Marcum Q-function	24
Pr	Probability	26
X^T	Transpose of X	34
X^H	Hermitian transpose of X	34
$\gamma(a, b)$	Lower incomplete gamma function	36

List of Abbreviations

Abbrv.	Definition	First Use
SNR	Signal-to-Noise Ratio	1
BER	Bit Error Rate	1
AF	Amount of Fading	1
LOS	Line-Of-Sight	3
PDF	Probability Density Function	3
RV	Random Variable	4
MRC	Maximal Ratio Combining	6
EGC	Equal Gain Combining	6
SC	Selection Combining	6
SD	Switched Diversity	6
GSC	Generalized Selection Combining	7
CDF	Cumulative Distribution Function	8
MGF	Moment Generating Function	8
ISR	Infinite Series Representation	9
CHF	Characteristic Function	9
MIMO	Multiple Input Multiple Output	12
AWGN	Additive White Gaussian Noise	25

Chapter 1

Introduction

Over the last two decades, we experienced a rapid advancement of telecommunication technologies. Wireless communication technologies can be considered as the main contributor for this rapid growth. Wireless communication, which started with Marconi's radio signals, has now evolved into wide variety of sophisticated technologies, and has taken over the role played by wired networks in voice and data communications. Demand for both fixed and mobile wireless services has grown exponentially over the past few years and according to recent surveys, there are more than four billion mobile wireless subscribers worldwide. The popularity of mobile wireless communications was boosted by the invention of small handheld devices such as smart phones and palmtop computers with wireless communication capabilities.

In the process of designing new wireless communication systems, the designer must make sure that the system is capable of functioning at a desirable level with a higher probability, under the impairments caused by the propagation channel. Performance measures such as average signal-to-noise ratio (SNR), average bit error rate (BER), outage probability and amount of fading (AF) are very popular quality indicators of wireless communication systems. Therefore it is quite beneficial to have a theoretical understanding on how the system performs with different configurations and different channel conditions. The impairments caused by the wireless propagation fall into several categories. Two major effects can be identified as multipath fading and shadowing. Several other impairments such as interference and jamming can also degrade the performance of wireless communication systems.

Due to the importance of the role played by performance evaluation in the system design process, it has been a popular research topic for more than five decades. It is evident from the large the number of research publications available on this topic. In this thesis,

we mainly focus on performance analysis of wireless communication systems, where the impairments are caused by multipath fading. We provide some important theoretical tools which can greatly reduce the complexity of performance evaluation of wireless communication systems. In the remaining discussion of this chapter, we provide a brief background on the topics discussed in this thesis. From Chapter 2 onwards, we present our results.

1.1 Multipath Fading

Signal (radiowave) propagation in a wireless medium is a complicated process. A signal propagating in a wireless medium may undergo several phenomenon such as scattering, reflection, refraction, and diffraction. Therefore the received signal at the receiver may consist of constructive and destructive combination of randomly scattered, delayed and reflected versions of the transmitted signal. This may result in random fluctuations of the received signal amplitude or power at the receiver. This entire process is referred to as multipath fading in wireless communications. Random variations of received signal amplitude and signal phase may result from multipath fading.

Depending on the type of signals used and the characteristics of the propagation channel, fading can be categorized into several forms. The relation between symbol duration and coherence time of the channel, defines two forms of fading, namely slow fading and fast fading. Coherence time is defined as the time period where we can consider the fading process is correlated. Slow fading occurs when the symbol duration is less than the channel coherence time. And fast fading is vice versa. Similarly another two forms of multipath fading can be identified as flat fading and frequency selective fading. These two types are defined based on the relation between channel coherence bandwidth and the transmitted signal bandwidth. Coherence bandwidth is defined as the frequency range over which the fading process is correlated. If the transmitted signal bandwidth is much smaller than the channel coherence bandwidth, the fading is considered to be flat and otherwise it is frequency selective.

In this thesis we consider the cases where the fading process is both slow and flat. When the multipath fading process satisfies these properties, it is common to use statistical distributions to model the random nature of the received signal amplitude. The basic and most widely used distributions include the Rayleigh distribution, Rician distribution, Nakagami-m distribution, Nakagami-q (Hoyt) distribution, and Weibull distribution.

1.1.1 Rayleigh fading

The Rayleigh distribution is often used to model the time varying characteristics of the received signal amplitude in a wireless channel where there is no direct line-of-sight (LOS) path between the transmitter and the receiver. The probability density function (PDF) of the Rayleigh distribution is given by

$$f_\alpha(x) = \frac{x}{\sigma^2} \exp\left(-\frac{x^2}{2\sigma^2}\right), \quad x \geq 0 \tag{1.1}$$

where $2\sigma^2$ is the mean square value of the received signal amplitude.

1.1.2 Rician fading

When a dominant signal component (eg: LOS component) is present in addition to the weaker multipath signals, the randomness of the received signal amplitude is modeled using the Rician distribution with the PDF given as

$$f_\alpha(x) = \frac{x}{\sigma^2} \exp\left(-\frac{x^2+\mu^2}{2\sigma^2}\right) I_0\left(\frac{\mu x}{\sigma^2}\right), \quad x \geq 0 \tag{1.2}$$

where $I_0(\cdot)$ is the modified Bessel function of first kind and zeroth order, and μ^2 is the power of the dominant component. The mean-square value of the signal amplitude of a Rician faded signal is given by $\mu^2 + 2\sigma^2$.

1.1.3 Nakagami-*m* fading

Nakagami-*m* model, first proposed in [1] is a more versatile distribution used to model multipath fading in wireless channels. It has shown a better fit for empirical data than Rayleigh and Rician distributions. The PDF of the Nakagami-*m* distribution is given by

$$f_\alpha(x) = \frac{2}{\Gamma(m)} \left(\frac{m}{\Omega}\right)^m x^{2m-1} \exp\left(-\frac{mx^2}{\Omega}\right), \quad x \geq 0, m \geq 0.5 \tag{1.3}$$

where $\Gamma(\cdot)$ is the Gamma function, and Ω is the mean square value of the amplitude. The fading severity parameter m is given by $\Omega^2/\mathbb{E}[(\alpha^2 - \Omega^2)]$, where $\mathbb{E}[\cdot]$ denotes the expectation of a random variable. For $m = 1$, the Nakagami-*m* distribution simplifies to the Rayleigh distribution and $m = 0.5$ represents the one-sided Gaussian distribution. As the value of the parameter m increases, the fading severity decreases.

1.1.4 Nakagami-*q* fading

Signal envelopes which closely follow the Nakagami-*q* (Hoyt) distribution [1], [2] have been observed in satellite links subject to strong scintillation [3]. The PDF of a Nakagami-*q* distributed random variable (RV) can be written as

$$f_\alpha(x) = \frac{(1+q^2)x}{q\Omega} \exp\left(-\frac{(1+q^2)^2x^2}{4q^2\Omega}\right) I_0\left(\frac{(1-q^4)x^2}{4q^2\Omega}\right), \quad x \geq 0 \tag{1.4}$$

where q is the Hoyt parameter which ranges from 0 to 1 and $\Omega = \mathbb{E}[\alpha^2]$. When $q = 1$, the Hoyt distribution simplifies to the Rayleigh distribution.

1.1.5 Weibull fading

The Weibull distribution was first introduced for the purpose of estimating the lifetime of machinery. It has several other applications such as reliability engineering, failure data analysis and weather forecasting. Several studies have shown that the Weibull distribution seems to be a good fit for experimentally measured fading channels in both indoor and outdoor environments [4], [5]. The PDF of the Weibull distribution can be written as [6]

$$f_\alpha(x) = \frac{\beta}{\gamma} x^{\beta-1} \exp\left(-\frac{x^\beta}{\gamma}\right), \quad x \geq 0, \beta > 0 \tag{1.5}$$

where β is the Weibull fading parameter, which determines the severity of fading, and γ is a positive scale factor which is related to moments of α such that $\gamma = \mathbb{E}[\alpha^\beta]$.

Some recent studies [7], [8] have developed statistical distributions with more degrees of freedom to model the multipath fading process, namely the $\alpha - \mu$ distribution, $\kappa - \mu$ distribution, and $\eta - \mu$ distribution. The basic fading distributions introduced above represent some special cases of these general fading distributions given in [7], [8]. Composite fading models have been introduced that can model the combined effects of multipath fading and shadowing with one tractable distribution. The K-distribution [9] and the generalized K-distribution fall in to this category.

1.2 Diversity Methods

Multipath fading and diversity methods are closely related topics in wireless communications. The diversity concept was introduced to countermeasure the detrimental effects of multipath fading on wireless communication system performance. The basic idea is to receive multiple independent versions of the transmitted signal and apply some processing

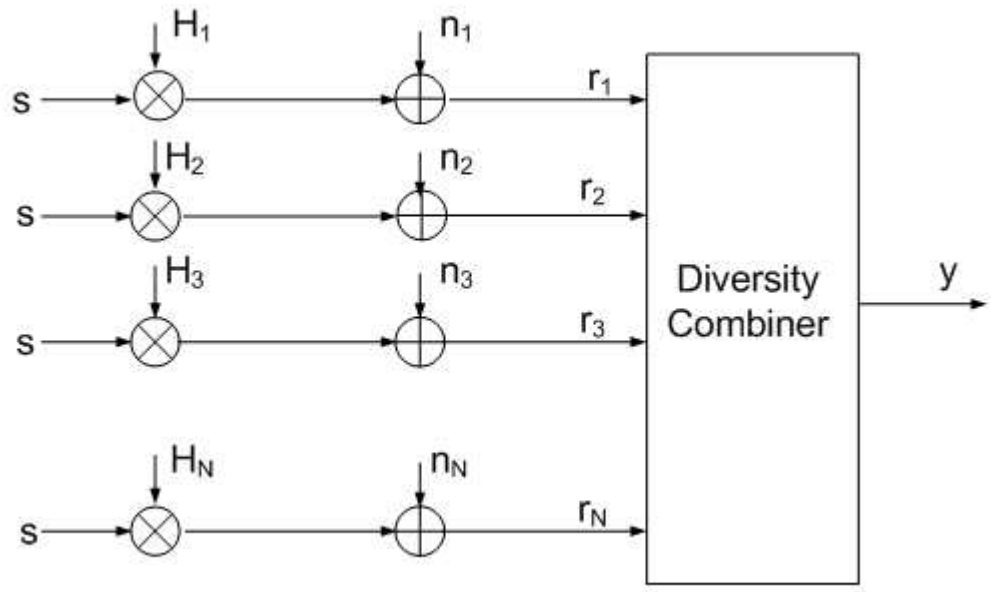

Figure 1.1. System model for a wireless communication system with diversity combiner.

algorithm at the receiver to obtain the decision statistic for decoding. The intuition under this concept is to exploit the low probability that multiple independent copies of the transmitted signal undergo a deep fade at the same time. The independence of the received signals may be achieved with several different techniques.

- In the spatial domain, using multiple receiver antennas
- In the frequency domain, using multiple frequency channels
- In the time domain, using multiple time slots
- Resolving multipath components at different delays (in wideband wireless systems)

In this thesis, we focus only on the diversity in the spatial domain with multiple receiver antennas. A basic system model for a wireless communication system with diversity combining is given in Fig.1.1. The effect of multipath fading $H_i, i \in (1, 2, \cdots, N)$ is modeled as a multiplicative effect on the transmitted signal $\mathbf{s}$. The additive noise is given as $n_i, i \in (1, 2, \cdots, N)$. The variables $r_i, i \in (1, 2, \cdots, N)$ denote the received signals at each receiver antenna. The symbol y denotes the output of the diversity combiner, which is used for symbol detection.

The four principal diversity combining techniques can be identified as follows.

1.2.1 Maximal ratio combining

Maximal ratio combining (MRC), is known as the optimal diversity combiner in the sense of maximizing the SNR of the decision statistic, in the absence of other interfering sources. In MRC, the received signals of each antenna (branch) are cophased and optimally weighted to obtain the combiner output. It has been shown that the SNR of the combiner output is equal to the summation of the SNR of all the branches. However, MRC requires complete channel state information (both channel gain amplitude and phase) of all the diversity branches to perform combining, and hence it is known to be the most complex diversity combiner.

1.2.2 Equal gain combining

In equal gain combining (EGC), the received signals of the branches are only cophased and added together to obtain the combiner output. It is a sub-optimal scheme compared to MRC, yet results in comparable performance with a lower complexity since only the knowledge of channel phase is required for combining. EGC is often limited in practice to coherent modulations with equal energy symbols.

1.2.3 Selection combining

In selection combining (SC), the receiver selects the branch with the highest instantaneous SNR for symbol decoding. Since SC processes only a single branch, it has a much lower complexity compared to MRC and EGC. However SC may not exploit the full diversity offered by the channel. SC can be used with coherent modulations (on a packet or block basis rather than on a symbol basis), noncoherent modulations and differentially coherent modulations.

1.2.4 Switched diversity combining

SC may not be suitable for communication systems with continuous transmissions, since it requires concurrent and continuous monitoring of all the branches. Switched diversity (SD) was proposed to overcome this limitation. In SD, the receiver selects a particular branch and remains with that branch until the SNR falls below a pre-determined threshold. Whenever the current branch SNR falls below a specified threshold, the receiver switches to another branch.

In addition to these principal combining techniques, several hybrid combining techniques have been proposed. These techniques were often developed such that they have characteristics of two or more principal combining algorithms. The purpose of hybrid combining techniques is to obtain maximum possible diversity benefit, while maintaining a reasonable receiver complexity. Generalized selection combining (GSC) was introduced by combining MRC with SC. In GSC, the receiver selects the strongest L branches out of N available branches, and combines the selected branches using MRC.

1.3 Fading Correlation Models

As mentioned in Section 1.2, independence of the multiple signal replicas at the branches is quite important to obtain the maximum benefit out of a diversity combiner. However satisfying this condition may be difficult in practical situations. In spatial diversity systems, it is known that the multiple receiver antennas should be placed sufficiently distant from each other to obtain independently faded signals at the antennas. As the wireless devices become smaller in size, implementing sufficiently spaced multiple antennas at the receiver may not be always possible. When this situation occurs, the fading conditions may be correlated among the multiple receiver antennas.

Theoretical performance evaluation of diversity combiners is an important stage in wireless system design. In order to choose a suitable combining scheme, a system designer should have a sound knowledge of the achievable performance of diversity combiners under different conditions. In order to study the performance using a realistic framework, we must include the effects of fading correlation in our theoretical analysis. To make the task analytically tractable, different fading correlation models have been introduced. The most widely used correlation models in the wireless communications literature include the exponential correlation model and the constant correlation model.

1.3.1 Exponential correlation model

The exponential correlation model, discussed in [10], is used to model the spatial fading correlation of an antenna system with equally spaced antennas. A uniform linear array is an example for an equally spaced set of antennas. This model assumes that the correlation between the pairs of received signals, decays as the spacing between antennas increases. The fading correlation coefficient between i^{th} and j^{th} receiver antennas is given as

$$\rho_{ij} = \rho^{|i-j|}, \quad 0 < \rho < 1, i \neq j \tag{1.6}$$

It is known that the covariance matrix of the exponential correlation model has tri-diagonal inverse, which makes it a tractable mathematical model for analysis.

1.3.2 Constant correlation model

The constant correlation model [10] is considered to be valid for a set of closely placed diversity antennas. In [11], it has been shown that a three-element circular antenna array gives rise to constant correlation conditions. Also the constant correlation model may be used as a worst case performance benchmark for a set of antennas [12]. The normalized covariance matrix for the constant correlation model can be given as

$$\begin{bmatrix} 1 & \rho & \rho & \cdots & \rho \\ \rho & 1 & \rho & \cdots & \rho \\ \rho & \rho & 1 & \cdots & \rho \\ \vdots & \vdots & \vdots & \vdots & \vdots \\ \rho & \rho & \rho & \cdots & 1 \end{bmatrix} \tag{1.7}$$

where $0 < \rho < 1$.

1.3.3 Need for better correlation models

In addition to these models, several attempts have been made to include arbitrary correlation conditions in theoretical analysis. The main difficulty that arises when we are dealing with performance evaluation of systems with fading correlation is that we have to use the joint fading statistics over the diversity branches. Generally it is extremely difficult to evaluate the joint statistics, since we must know the mathematical representations for the joint statistical distributions for the prevailing correlation conditions. For an example, performance analysis of selection diversity receivers in correlated fading channels generally requires the joint cumulative distribution function (CDF) of the branch SNRs. Also the analysis of EGC in correlated fading channels requires the joint PDF of the received signal envelopes. For MRC receivers, the joint moment generating function (MGF) of the branch SNRs is preferred.

Since the performance evaluation of diversity reception in the presence of fading correlation became an important research area in wireless communications, several researchers focused their attention on the problem of finding mathematically tractable forms for the multivariate PDF, CDF and MGF of the widely used statistical distributions such as Rayleigh, Rician, Nakagami-*m* and Weibull. In the following section, we present a summary of the

existing results on the multivariate PDF, CDF and MGF representations of these distributions.

1.4 Related Previous Results

In this section, we present some previous results available for representing the multivariate PDFs and CDFs of statistical distributions considered in this thesis.

A thorough analysis of multivariate PDFs and CDFs of statistical distributions derived from the Gaussian distribution is found in [13]. Using the methodology given in [13], multivariate probability distributions for the Rayleigh distribution were investigated in [14]. Special cases of the constant correlation model and the exponential correlation model were considered in the analysis of [14]. A closed-form multivariate PDF expression was derived for the exponential correlation case and the joint PDF for the constant correlation case was given in terms of a multidimensional integration requiring N levels of integration for a N dimensional distribution. An infinite series representation (ISR) for the bivariate Rayleigh CDF was first given in [15]. A finite range single integral representation for the bivariate Rayleigh distribution was given in [16].

There are limited results on multivariate PDF and CDF representations for the Rician distribution. The bivariate Rician PDF is given as an infinite summation in [17] – [19]. Extending Miller's approach [13], an infinite series representations of the PDF and CDF of the tri-variate Rician distribution, when the underlying Gaussian RVs have a tri-diagonal inverse covariance matrix, are given in [20] where the Rician PDF is expressed using 2 nested infinite summations while the CDF is given using 7 nested infinite summations. A useful single integral representation for the bivariate Rician PDF was given in [21], which was readily obtained from the results of [22].

Certain forms of multivariate probability distributions for the Nakagami-*m* distribution are found in the literature [1], [15], [23] – [28]. A closed-form representation of the bivariate Nakagami-*m* PDF was given in [1] for identical fading severity parameter *m* for both random variables (RVs). An infinite series representation of the bivariate Nakagami CDF, when the two RVs have identical *m* values was first published in [15]. The bivariate Nakagami PDF, with arbitrary fading parameters for the RVs, can be found in [23]. The authors of [26], generalized the results in [23], to represent more general correlation that may exist in real propagation channels. Infinite series representations for the joint characteristic function (CHF), PDF, and CDF were given for the bivariate Nakagami-*m* distribution using

generalized Laguerre polynomials. The trivariate Nakagami-*m* and Rayleigh distributions are known for arbitrary covariance matrices of the underlying Gaussian RVs [25], [27], [29] in forms where the PDF and CDF are represented using a single infinite summation. Also, quadri-variate Nakagami-*m* and Rayleigh distributions are given in [25], [29] for the most general case of covariance matrix for the underlying Gaussian RVs. The PDF and CDF are expressed as multiple nested infinite summations. A multivariate Nakagami-*m* distribution with exponential correlation among the underlying Gaussian RVs was presented in [24]. Reference [30] presented an efficient approach to obtain multivariate PDF and CDF representations for the Nakagami-*m* distribution, by approximating the covariance matrix of the RVs with a suitable Green's matrix. Since Green's matrix is guaranteed to have its inverse in tri-diagonal form, Miller's approach [13] can then be used to obtain the multivariate PDF and CDF. The multivariate Nakagami CDF was given using multiple nested infinite summations. An infinite series representation of a multivariate Nakagami-*m* PDF for arbitrary correlation matrix and arbitrary fading severity parameters was given in [28]. The PDF was given using a single infinite summation of Laguerre polynomials. The multivariate Nakagami-*m* CDF was given using a multidimensional integration of the PDF in [28]. A union upper bound for multivariate Nakagami-*m* fading model is given in [31].

The Rician distribution is a special case of the non-central chi (χ) distribution[1] where the number of degrees of freedom is equal to 2. An ISR for the bivariate generalized Rician distribution was given in [13]. Royen [32] gives integral representations for central and non-central multivariate chi-square (χ^2) distributions with specific correlation structures. An ISR for the PDF and CDF of the trivariate non-central χ^2 distribution is given in [33], where the inverse covariance matrix of the underlying Gaussian random variables (RVs) is in tri-diagonal form. Both the PDF and CDF are expressed using nested infinite summations. Reference [34] gives a new representation for the trivariate non-central χ^2 distribution derived from the diagonal elements of a complex non-central Wishart matrix.

Special forms of the multivariate Weibull fading process generated from correlated Gaussian processes were studied in [6]. A closed-form expression for the multivariate Weibull PDF with exponential correlation among the underlying Rayleigh RVs is given in [6]. A nested integral form of the multivariate PDF for the constant correlation model is also given in [6] for identically distributed Weibull RVs. A multivariate CDF is given for the exponential correlation case using multiple nested infinite summations. A CDF ex-

[1] If RV X is distributed as non-central χ^2 then the RV $\sqrt{X}$ is a non-central χ distributed RV.

pression for the constant correlation case was not given in [6]. The results of [6] were extended to arbitrary correlation conditions using a Green's matrix approximation in [35]. However the results are given in terms of multiple nested infinite summations and are not exact. Infinite series representations for the trivariate Weibull PDF and CDF with arbitrary correlations are given in [36] for the general case of non-identically distributed Weibull RVs. Reference [36] gives ISRs for the quadri-variate Weibull PDF and CDF with a very general correlation matrix. However, neither the PDF nor the CDF given in [36] for the quadri-variate Weibull distribution is valid for the constant correlation case. A general and exact multivariate PDF expression for the $\alpha - \mu$ distribution with arbitrary correlation is given in [37] where the Weibull distribution is considered as a special case of the $\alpha - \mu$ distribution. However, only an approximate solution is given for the multivariate CDF.

1.5 Motivation

Reviewing the existing literature on multivariate PDF and CDF representations of Rayleigh, Rician, Nakagami-*m*, non-central χ^2 and Weibull distributions, we notice the following.

- Despite their usefulness, there exist a limited number of multivariate PDF and CDF representations for Rayleigh, Rician, Nakagami-*m*, Weibull and non-central χ^2 distributions.
- When the multivariate PDF and CDF representations are available, their mathematical complexity precludes their use in certain applications.
- In some cases where the multivariate PDF is known, still we have to use multi-dimensional integration to evaluate the multivariate CDF.
- The majority of the known results on multivariate distributions are given in terms of infinite series solutions or multi-dimensional integral expressions, which are difficult and time consuming to evaluate using mathematical software.
- The number of infinite series computations or integral computations increases with the dimensionality of the distribution.
- The approximation methods used to obtain multivariate PDF and CDF representations become less accurate as the number of dimensions increases.

- The tightness of the known bounds for multivariate PDF and CDF representations tend to deteriorate as the distribution grows to higher dimensions.

Due to the availability of multivariate Gamma type MGFs for arbitrary correlation conditions, the performance of MRC receivers under arbitrary fading correlation conditions have been studied extensively for correlated Rayleigh, Rician and Nakagami-*m* fading channels. However, exact performance results available for SC receivers in correlated fading channels appear to be limited. Motivated by this fact and the limitations we identified earlier, in this thesis, we present a framework to derive conveniently computable mathematical representations for multivariate Rayleigh, Rician, Nakagami-*m*, non-central χ^2 and Weibull distributions. Special types of correlation models are used in our analysis. Although performance evaluation of SC receivers is a motivation for this thesis, it will be shown that the new results developed in this thesis can also be used in the analysis of multiple input multiple output (MIMO) systems with antenna selection and in the analysis of output SNR moments of EGC.

In addition to the new representations for the multivariate distributions, motivated by the fact that the available solutions for the performance analysis of a dual branch MRC receiver operating in correlated Hoyt fading channels are quite complicated in mathematical evaluation, we present a new simple methodology to tackle this problem as well.

1.6 Thesis Outline and Contributions

This thesis develops a simplified framework to derive multivariate PDF and CDF expressions for some popular statistical distributions used in wireless communications theory. Specific types of correlation matrices are used in our analysis. We focus our attention on deriving easily computable mathematical representations for multivariate distributions including Rayleigh, Rician, Nakagami-*m*, Weibull and non-central chi-square distributions[2]. This thesis consists of four main chapters. Each chapter corresponds to a major contribution.

Chapter 2 presents a framework to derive novel single integral solutions for multivariate PDFs and CDFs of Rayleigh, Rician and Nakagami-*m* distributions with generalized correlation structure. We show that our new methodology enables derivation of single integral expressions for multivariate PDFs and CDFs of Rayleigh, Rician and Nakagami-*m*

[2]For each case, with the aid of mathematical software such as MAPLE, we can show that the marginal distributions follow the appropriate forms

distributions with a generalized correlation matrix. The new PDF expressions are used to derive single integral expressions for joint moments. We use the new multivariate CDF representations to evaluate performance of SC diversity, operating in correlated Rayleigh, Rician and Nakagami-*m* fading channels.

In Chapter 3, we consider the special case of constant (equal) correlation model for our analysis. We derive new single integral representations for the multivariate non-central chi-square distribution with equally correlated component Gaussian RVs. The new representations are derived for the multivariate PDF, CDF, joint CHF and joint moments. Also we discuss the applicability of the new representations of the non-central chi-square distribution to study of MIMO systems with antenna selection, operating in correlated Rician fading channels.

Chapter 4 presents new single integral expressions for the multivariate Weibull distribution with constant correlation. New single integral expressions for the multivariate PDF, CDF and joint moments are derived. We use the new CDF representation to evaluate the performance of SC diversity operating in correlated Weibull fading channels. New expressions for the outage probability, average symbol error rate and average SNR are derived. Furthermore, the new PDF is used to obtain new expressions for the output SNR moments of EGC operating in equally correlated Weibull fading.

Chapter 5 presents a new framework to analyze the performance of a dual MRC receiver operating in identically distributed, correlated Nakagami-*q* (Hoyt) fading channels. The new method allows computing the SER of a large number of coherent and noncoherent modulation formats with dual MRC in correlated Hoyt fading using finite range single integrals of elementary mathematical functions. Also we show that this method allows computing other performance measures such as outage probability of the MRC receiver, using efficient numerical techniques developed for independent fading branches.

Chapter 6 concludes this thesis while giving some suggestions for potential future research based on the contributions of this thesis. It is important to note that although we discuss the applicability of the new representations of the multivariate distributions in wireless communications, the new distributions can be used in other areas of statistics as well.

Chapter 2

New Representations for Multivariate Rayleigh, Rician and Nakagami-*m* Distributions With Generalized Correlation

2.1 Introduction

In this chapter[1], we present a framework to obtain single integral representations for multivariate Rayleigh, Rician and Nakagami-*m* distributions with a generalized correlation structure. The multivariate PDFs and CDFs are expressed explicitly in terms of single integral solutions. A remarkable feature of these representations is that the computational complexity is limited to a single integral computation for an arbitrary number of dimensions. Correlated RVs are generated using a special transformation of independent Gaussian RVs. A similar approach was used in [12] to obtain distribution functions of the output signal-to-noise ratio (SNR) of a selection diversity combiner exclusively for equally correlated fading. In [40], this approach was used to evaluate performance of diversity combiners with positively correlated branches. Prior to the publication of [12] and [40], the basic idea for the approach was found in [41]. Our model is two-dimensional as is the model in [12], [40], and admits some negative values of correlation as does the most general model in [41].

The remainder of this chapter is organized as follows. In Section 2.2, we present models used to generate correlated Rayleigh, Rician and Nakagami-*m* distributed RVs from independent Gaussian RVs. Detailed derivations of multivariate Rayleigh, Rician and Nakagami-*m* distributions are presented in Section 2.3. Section 2.4 presents applica-

[1]This chapter has been presented in part at the IEEE Wireless Communications and Networking Conference (WCNC) 2010, held in Sydney, Australia [38], [39].

tions of the new representations, while some numerical examples and simulation results are presented in Section 2.5.

2.2 Representation of Correlated RVs

The following notations will be used throughout this chapter and the remainder of this thesis. We denote a Gaussian distribution with mean μ and variance σ^2 by $\mathcal{N}(\mu, \sigma^2)$, and a complex Gaussian distribution with mean μ and variance σ^2 is denoted as $N_c(\mu, \sigma^2)$. Var$(\cdot)$ denotes the variance of a RV, and the magnitude and complex conjugate of X are denoted as $|X|$ and X^*, respectively. We use $f_X(x)$ and $F_X(x)$ to denote the PDF and CDF of RV X.

2.2.1 Correlated Rayleigh RVs

Similar to [40, eq.(6)], the complex channel gain can be represented by extending the correlation model used in [41, eq.(8.1.6)] to the complex plane as

$$G_k = (\sqrt{1-\lambda_k^2}X_k + \lambda_k X_0) + i(\sqrt{1-\lambda_k^2}Y_k + \lambda_k Y_0), \quad k = 1, \cdots, N \tag{2.1}$$

where $i = \sqrt{-1}$, $\lambda_k \in (-1, 1) \setminus \{0\}$ and $X_k, Y_k (k = 0, \cdots, N)$ are independent and $\mathcal{N}(0, \frac{1}{2})$. Then for any $k, j \in \{0, \cdots, N\}$, $\mathbb{E}[X_k Y_j] = 0$, and $\mathbb{E}[X_k X_j] = \mathbb{E}[Y_k Y_j] = \frac{1}{2}\delta_{kj}$ where δ_{kj} is the Kronecker delta function defined as $\delta_{kk} = 1$ and $\delta_{kj} = 0$ for $k \neq j$.

Then G_k has a zero-mean complex Gaussian distribution as $N_C(0, 1)$, and $|G_k|$ is Rayleigh distributed with mean square value $\mathbb{E}[|G_k|^2] = 1$. The cross-correlation coefficient between any G_k, G_j can be calculated as

$$\rho_{kj} = \frac{\mathbb{E}[G_k G_j^*] - \mathbb{E}[G_k]\mathbb{E}[G_j^*]}{\sqrt{\mathbb{E}[|G_k|^2]\mathbb{E}[|G_j|^2]}} = \lambda_k \lambda_j. \tag{2.2}$$

Observe that (2.1) can generate correlated Rayleigh RVs with the underlying complex Gaussian RVs having the cross-correlation structure given in (2.2). The corresponding envelope correlations can be found using [42, eq. (1.5-26)]. When all $\lambda_k = \lambda, (k = 1, \cdots, N)$, this model simplifies to the equal correlation case.

2.2.2 Correlated Rician RVs

We can denote a set of correlated Rician RVs by modifying the correlation model used in (2.1), namely

$$H_k = (\sqrt{1-\lambda_k^2}X_k + \lambda_k X_0) + i(\sqrt{1-\lambda_k^2}Y_k + \lambda_k Y_0), \quad k = 1, \cdots, N \tag{2.3}$$

where $i = \sqrt{-1}$, $\lambda_k \in (-1,1) \setminus \{0\}$ and $X_k, Y_k (k = 1, \cdots, N)$ are independent and $\mathcal{N}(0, \frac{1}{2})$. The RVs X_0 and Y_0 are independent and distributed as $\mathcal{N}(m_1, \frac{1}{2})$ and $\mathcal{N}(m_2, \frac{1}{2})$. Then for any $k, j \in \{1, \cdots, N\}$, $\mathbb{E}[X_k Y_j] = 0$, and $\mathbb{E}[X_k X_j] = \mathbb{E}[Y_k Y_j] = \frac{1}{2}\delta_{kj}$.

Note that H_k is a non-zero mean complex Gaussian distributed RV, and $|H_k|$ is Rician distributed with Rician factor $K_k = \lambda_k^2(m_1^2 + m_2^2)$ and mean square value $\mathbb{E}[|H_k|^2] = 1 + K_k$. The cross-correlation coefficient between any H_k, H_j can be calculated as

$$\rho_{kj} = \frac{\mathbb{E}[H_k H_j^*] - \mathbb{E}[H_k]\mathbb{E}[H_j^*]}{\sqrt{\mathbb{E}[|H_k - \mathbb{E}[H_k]|^2]\,\mathbb{E}[|H_j - \mathbb{E}[H_j]|^2]}} = \lambda_k \lambda_j. \tag{2.4}$$

Therefore, (2.3) can represent correlated Rician RVs with the underlying complex Gaussian RVs having the cross-correlation structure given in (2.4) . When all $\lambda_k = \lambda (k = 1, \cdots, N)$, this model simplifies to the equal correlation case.

2.2.3 Correlated Nakagami-*m* RVs

Modifying the model described in [41], we can denote N correlated Nakagami-*m* (for positive integer m) random variables with Nm number of zero-mean complex Gaussian random variables. Using a similar approach as [40],

$$G_{kl} = \sigma_k(\sqrt{1-\lambda_k^2} X_{kl} + \lambda_k X_{0l}) + i\,\sigma_k(\sqrt{1-\lambda_k^2} Y_{kl} + \lambda_k Y_{0l}) \\ k = 1, \cdots, N \;\; l = 1, \cdots, m \tag{2.5}$$

where $i = \sqrt{-1}$, $\lambda_k \in (-1,1)\backslash\{0\}$ and $X_{kl}, Y_{kl} (k = 0, 1, \cdots, N \;\; l = 1, \cdots, m)$ are independent and $\mathcal{N}(0, \frac{1}{2})$. Then for any $k, j \in \{1, \cdots, N\}$, $l, n \in \{1, \cdots, m\}$, $\mathbb{E}[X_{kl} Y_{jn}] = 0$, and $\mathbb{E}[X_{kl} X_{jn}] = \mathbb{E}[X_{kl} Y_{jn}] = \dfrac{1}{2}\delta_{kj}\delta_{ln}$. The cross-correlation coefficient between any G_{kl} and G_{jn} $(k \neq j)$ can be calculated as

$$\begin{aligned} \rho_{kl,jn} &= \frac{\mathbb{E}[G_{kl} G_{jn}^*] - \mathbb{E}[G_{kl}]\mathbb{E}[G_{jn}^*]}{\sqrt{\mathbb{E}[|G_{kl}|^2] \;\; \mathbb{E}[|G_{jn}|^2]}} \\ &= \begin{cases} \lambda_k \lambda_j & (k \neq j \; and \; l = n) \\ 0 & (l \neq n). \end{cases} \end{aligned} \tag{2.6}$$

Denote R_k as the summation of squared magnitudes of G_{kl}, then

$$R_k = \sum_{l=1}^{m} |G_{kl}|^2. \tag{2.7}$$

$R_k (k = 1, \cdots, N)$ is sum of squares of $2m$ independent Gaussian RVs. The cross-correlation coefficient between R_k and R_j can be calculated as [1]

$$\rho_{R_k, R_j} = \frac{\mathbb{E}[R_1 R_2^*] - \mathbb{E}[R_1]\mathbb{E}[R_2^*]}{\sqrt{\text{Var}[R_1]\text{Var}[R_2]}} = \lambda_k^2 \lambda_j^2. \tag{2.8}$$

We identify that $\sqrt{(}R_k)(k = 1, \cdots, N)$ are a set of N correlated Nakagami-*m* RVs with mean square value $m\sigma_k^2$, identical fading severity parameter m and cross-correlation of the underlying complex Gaussian RVs having the structure given in (2.6).

2.3 Multivariate Rayleigh, Rician and Nakagami-*m* Distributions

2.3.1 Multivariate Rayleigh distribution

In Section 2.2.1, it was shown that the $|G_k|$s are Rayleigh distributed. We condition the RVs $|G_k|$s on the RVs X_0 and Y_0. Then we identify that the $|G_k|$s become conditionally Rician distributed since the inphase and quadrature components have equal variances and non-zero means. The PDF of $|G_k|$ conditioned on X_0 and Y_0 can be written as [43]

$$f_{|G_k||X_0,Y_0}(r_k|X_0,Y_0) = \frac{r_k}{\sigma_k^2}\exp\left(-\frac{(r_k^2+\mu_k^2)}{2\sigma_k^2}\right) I_0\left(\frac{r_k\mu_k}{\sigma_k^2}\right) \tag{2.9a}$$

$$\mu_k^2 = \mu_x^2 + \mu_y^2 \tag{2.9b}$$

$$\mu_x = \lambda_k X_0 \tag{2.9c}$$

$$\mu_y = \lambda_k Y_0 \tag{2.9d}$$

$$\sigma_k^2 = \frac{1-\lambda_k^2}{2}, \quad k = 1, \cdots, N. \tag{2.9e}$$

One can compute the conditional cross-correlation coefficient between G_k and G_j using

$$\rho_{kj}^c = \frac{\mathbb{E}[G_k G_j^*|X_0,Y_0] - \mathbb{E}[G_k|X_0,Y_0]\mathbb{E}[G_j^*|X_0,Y_0]}{\sqrt{\mathbb{E}[|G_k - \mathbb{E}[G_k]|^2|X_0,Y_0]\,\mathbb{E}[|G_j - \mathbb{E}[G_j]|^2|X_0,Y_0]}} = 0. \tag{2.10}$$

The conditional G_ks are uncorrelated. Since they are Gaussian distributed, they are conditionally independent. Therefore, the $|G_k|$s are conditionally independent, and the joint conditional PDF of the $|G_k|$s can be written as

$$f_{\mathbf{G}|X_0,Y_0}(r_1, r_2, \cdots, r_N|X_0,Y_0) = \prod_{k=1}^{N} f_{|G_k||X_0,Y_0}(r_k|X_0,Y_0) \tag{2.11}$$

where $f_{|G_k|}(r_k|X_0,Y_0)$ is given in (2.9) and $\mathbf{G} = [|G_1|, \cdots, |G_N|]$.

From the laws of probability we know that [44]

$$f_G(r_1, r_2, r_3, \cdots, r_N) = \int_{Y_0}\int_{X_0} f_{\mathbf{G},X_0,Y_0}(r_1, r_2, \cdots, r_N, X_0, Y_0)\ \ dX_0 dY_0. \tag{2.12}$$

Also we have

$$f_{\mathbf{G},X_0,Y_0}(r_1, r_2, \cdots, r_N, X_0, Y_0) = f_{\mathbf{G}|X_0,Y_0}(r_1, r_2, \cdots, r_N|X_0, Y_0) \;\; f_{X_0,Y_0}(X_0, Y_0). \tag{2.13}$$

Then we can write the unconditional joint PDF as

$$f_{\mathbf{G}}(r_1, r_2, r_3, \cdots, r_N) = \int_{Y_0}\int_{X_0} f_{\mathbf{G}|X_0,Y_0}(r_1, r_2, \cdots, r_N|X_0, Y_0) \;\; f_{X_0,Y_0}(X_0, Y_0) \;\; dX_0 dY_0. \tag{2.14}$$

Since X_0, Y_0 are independent and $\mathcal{N}(0, \frac{1}{2})$, the joint PDF is given by

$$f_{X_0,Y_0}(X_0, Y_0) = \frac{1}{\pi}\exp(-(X_0^2 + Y_0^2)). \tag{2.15}$$

Then we can write the joint unconditional PDF of correlated Rayleigh RVs as

$$f_{\mathbf{G}}(r_1, r_2, \cdots, r_N) = \int_{Y_0}\int_{X_0} \prod_{k=1}^{N} f_{|G_k|}(r_k|X_0, Y_0) \;\; \frac{1}{\pi}\exp(-(X_0^2 + Y_0^2)) \;\; dX_0 dY_0. \tag{2.16}$$

Substituting (2.9) in (2.16), and using some straightforward variable transformations, we simplify the double integral in (2.16) to a single integral, namely

$$f_{\mathbf{G}}(r_1, r_2, \cdots, r_N) = \int_0^{\infty} \exp(-t) \prod_{k=1}^{N} \frac{r_k}{\sigma_k^2} \exp\left(-\frac{r_k^2 + \lambda_k^2 t}{2\sigma_k^2}\right) I_0\left(\frac{r_k\sqrt{\lambda_k^2 t}}{\sigma_k^2}\right) \;\; dt. \tag{2.17}$$

Eq. (2.17) is a new single integral form of a class of multivariate Rayleigh distributions, the class admitted by the correlation structure given in (2.2). In comparison to other special forms of the multivariate Rayleigh distribution, we make the following remarks. Only a single integral calculation is needed to compute the N-dimensional multivariate Rayleigh PDF (2.17) having the correlation structure given in (2.2). No multiple nested infinite series computations are required, in sharp contrast to previously published forms of the PDF [15], [29]. In comparison to the result in [14], N-fold integration is required in [14], but the solution is valid for arbitrary correlation.

The bivariate Rayleigh PDF is well known [45]. One can show that (2.17) specializes to this known form using [46, eq. (3.15.17.1)] as

$$f_{|G_1|,|G_2|}(r_1, r_2) = \frac{4r_1 r_2}{1-\lambda}\exp\left(-\frac{1}{1-\lambda}\left(r_1^2 + r_2^2\right)\right) I_0\left(\frac{2r_1 r_2\sqrt{\lambda}}{1-\lambda}\right) \tag{2.18}$$

where the correlation coefficient $\rho = \lambda_1^2\lambda_2^2$, can have arbitrary value $0 \leq \rho < 1$.

We obtain a single integral representation for the multivariate Rayleigh CDF using the same approach. We write

$$F_{\mathbf{G}}(r_1, r_2, r_3, \cdots, r_N) = \int_{Y_0}\int_{X_0} F_{\mathbf{G}|X_0,Y_0}(r_1, r_2, \cdots, r_N|X_0, Y_0)\ f_{X_0,Y_0}(X_0, Y_0)\ \ dX_0 dY_0 \quad (2.19)$$

where $F_{\mathbf{G}|X_0,Y_0}(r_1, r_2, \cdots, r_N|X_0, Y_0)$ is given by [43]

$$F_{\mathbf{G}|X_0,Y_0}(r_1, r_2, \cdots, r_N|X_0, Y_0) = \prod_{k=1}^{N}\left[1 - Q\left(\frac{\mu_k}{\sigma_k}, \frac{r_k}{\sigma_k}\right)\right] \quad (2.20)$$

and $Q(a, b)$ is the 1st order Marcum Q-function [43] and μ_k and σ_k are as defined in 2.9. Then we can write the joint CDF as a single integral, namely

$$F_{\mathbf{G}}(r_1, r_2, \cdots, r_N) = \int_0^{\infty} \exp(-t) \prod_{k=1}^{N}\left[1 - Q\left(\frac{\sqrt{t}\sqrt{\lambda_k^2}}{\sigma_k}, \frac{r_k}{\sigma_k}\right)\right] dt. \quad (2.21)$$

Eq. (2.21) for the multivariate Rayleigh CDF was published previously in [40], with the difference that in [40], it was specified that the λ_k, $k = 1, \cdots, N$ must be positive whereas the derivation given here allows negative and positive values for λ_k.

2.3.2 Multivariate Rician distribution

In Section 2.2.2, a model for Rician distributed $|H_k|$ was given. Now we condition H_k on random variables X_0 and Y_0. Then we can identify that $|H_k|$ is still Rician distributed since the inphase and quadrature components have equal variances and non-zero means. The PDF of $|H_k|$ conditioned on X_0 and Y_0 can be written as [43]

$$f_{|H_k||X_0,Y_0}(v_k|X_0, Y_0) = \frac{v_k}{\sigma_k^2}\exp(-\frac{(v_k^2 + S_k^2)}{2\sigma_k^2})I_0(\frac{v_k S_k}{\sigma_k^2}) \quad (2.22a)$$

$$S_k^2 = \mu_x^2 + \mu_y^2 \quad (2.22b)$$

$$\mu_x = \lambda_k X_0, \mu_y = \lambda_k Y_0 \quad (2.22c)$$

$$\sigma_k^2 = \frac{1 - \lambda_k^2}{2}, \quad k = 1, \cdots, N. \quad (2.22d)$$

One can compute the conditional cross-correlation coefficient between H_k and H_j using

$$\rho_{k,j}^c = \frac{\mathbb{E}[H_k H_j^*|X_0, Y_0] - \mathbb{E}[H_k|X_0, Y_0]\mathbb{E}[H_j^*|X_0, Y_0]}{\sqrt{\mathbb{E}[|H_k - \mathbb{E}[H_k]|^2|X_0, Y_0]\,\mathbb{E}[|H_j - \mathbb{E}[H_j]|^2|X_0, Y_0]}} = 0. \quad (2.23)$$

The conditional H_k's are uncorrelated. Since they are jointly Gaussian, they are conditionally independent. Therefore, we can write the joint conditional PDF of the $|H_k|$'s as

$$f_{\mathbf{H}|X_0,Y_0}(v_1, v_2, \cdots, v_N|X_0, Y_0) = \prod_{k=1}^{N} f_{|H_k||X_0,Y_0}(v_k|X_0, Y_0) \tag{2.24}$$

where $f_{|H_k||X_0,Y_0}(v_k|X_0, Y_0)$ is given in (2.22) and $\mathbf{H} = [|H_1|, \cdots, |H_N|]$.

Reasoning as the Rayleigh case, we can write the unconditional joint PDF as

$$f_{\mathbf{H}}(v_1, v_2, v_3, \cdots, v_N) = \int_{Y_0}\int_{X_0} f_{\mathbf{H}|X_0,Y_0}(v_1, v_2, \cdots, v_N|X_0, Y_0)\ f_{X_0,Y_0}(X_0, Y_0)\ dX_0 dY_0. \tag{2.25}$$

Since X_0, Y_0 are independent and distributed as $\mathcal{N}(m_1, \frac{1}{2})$ and $\mathcal{N}(m_1, \frac{1}{2})$, the joint PDF is

$$f_{X_0,Y_0}(X_0, Y_0) = \frac{1}{\pi}\exp(-((X_0 - m_1)^2 + (Y_0 - m_2)^2)). \tag{2.26}$$

Then we can write the joint unconditional PDF of correlated Rician RVs as

$$f_{\mathbf{H}}(v_1, v_2, \cdots, v_N) = \int_{-\infty}^{\infty}\int_{-\infty}^{\infty} \frac{1}{\pi}\exp(-((X_0 - m_1)^2 + (Y_0 - m_2)^2)) \prod_{k=1}^{N} \frac{v_k}{\sigma_k^2}\exp\left(-\frac{v_k^2 + \lambda_k^2(X_0^2 + Y_0^2)}{2\sigma_k^2}\right) I_0\left(\frac{v_k\sqrt{\lambda_k^2(X_0^2 + Y_0^2)}}{\sigma_k^2}\right) dX_0 dY_0. \tag{2.27}$$

Using the variable transformation $X_0 = Rcos(\theta)$ and $Y_0 = Rsin(\theta)$, we can simplify (2.27) to a single integral, namely

$$f_{\mathbf{H}}(v_1, v_2, \cdots, v_N) = \int_0^{\infty} \exp(-t)\exp(-(m_1^2 + m_2^2))I_0(2\sqrt{(m_1^2 + m_2^2)t}) \prod_{k=1}^{N} \frac{v_k}{\sigma_k^2}\exp\left(-\frac{v_k^2 + \lambda_k^2 t}{2\sigma_k^2}\right) I_0\left(\frac{v_k\sqrt{\lambda_k^2 t}}{\sigma_k^2}\right) dt. \tag{2.28}$$

Eq. (2.28) is a new representation of a class of multivariate Rician PDF with the correlation structure given in (2.3). Only a single integral is needed to compute the N-dimensional Rician PDF (2.28) having the correlation structure given in (2.4). Multiple nested infinite summations are not required to compute the N-dimensional Rician PDF. Also, we will show that the CDF can be obtained in single integral form as well.

We obtain a single integral representation of the multivariate Rician CDF using a similar approach by replacing $f_{\mathbf{H}|X_0,Y_0}(v_1, v_2, \cdots, v_N|X_0, Y_0)$ by $F_{\mathbf{H}|X_0,Y_0}(v_1, v_2, \cdots, v_N|X_0, Y_0)$, which is given by

$$F_{\mathbf{H}|X_0,Y_0}(v_1, v_2, \cdots, v_N|X_0, Y_0) = \prod_{k=1}^{N}\left[1 - Q\left(\frac{S_k}{\sigma_k}, \frac{v_k}{\sigma_k}\right)\right]. \tag{2.29}$$

Then we can represent the multivariate Rician CDF as

$$F_{\mathbf{H}}(v_1, v_2, \cdots, v_N) = \int_0^\infty \exp(-t)\exp(-(m_1^2+m_2^2))I_0\left(2\sqrt{t}\sqrt{m_1^2+m_2^2}\right) \times \prod_{k=1}^{N}\left[1 - Q\left(\frac{\sqrt{t}\sqrt{\lambda_k^2}}{\sigma_k}, \frac{v_k}{\sigma_k}\right)\right] dt. \quad (2.30)$$

Eq. (2.30) is a new representation for a multivariate Rician CDF. Only a single integral computation is required to evaluate the N-dimensional Rician CDF with correlation structure given in (2.3). No multiple nested infinite summations are required for computation, in contrast to the forms given in [17] and [25].

2.3.3 Multivariate Nakagami-*m* distribution

A model to generate correlated Nakagami-*m* RVs was given in (2.5). Now we condition the RV's G_{kl} on X_{0l} and Y_{0l} for $l = 1, \cdots, m$. Then the real and imaginary parts of G_{kl} have equal variance of $\sigma_k^2\left(\frac{1-\lambda_k^2}{2}\right)$ and means $\sigma_k\lambda_k X_{0l}$ and $\sigma_k\lambda_k Y_{0l}$, respectively. We can identify that R_k has a noncentral chi-square distribution $\chi_{2m}(S_k, \Omega_k^2)$ where $S_k^2 = \sum_{l=1}^{m}\sigma_k^2\lambda_k^2(X_{0l}^2 + Y_{0l}^2)$ and $\Omega_k^2 = \sigma_k^2\left(\frac{1-\lambda_k^2}{2}\right)$. We can write the conditional PDF of R_k as [43]

$$f_R(\gamma|X_{0l}, Y_{0l}) = \frac{1}{2\Omega_k^2}\left(\frac{\gamma}{S_k^2}\right)^{\frac{2m-2}{4}}\exp(-\frac{(S_k^2+\gamma)}{2\Omega_k^2})\ I_{\frac{2m}{2}-1}\left(\sqrt{\gamma}\frac{S_k}{\Omega_k^2}\right). \quad (2.31)$$

We can find the conditional PDF of $\sqrt{R_k}$ using a variable transformation; it is given by

$$f_{\sqrt{R_k}}(w_k|X_{0l}, Y_{0l}) = \frac{1}{\Omega_k^2}\frac{w_k^m}{S_k^{m-1}}\exp(-\frac{(S_k^2+w_k^2)}{2\Omega_k^2})\ I_{m-1}\left(w_k\frac{S_k}{\Omega_k^2}\right). \quad (2.32)$$

Since the components G_{kl} are conditionally independent on X_{0l} and Y_{0l}, the resulting R_k's are independent for $k = 1, \cdots, N$. Then the conditional joint PDF of the resulting $\sqrt{R_k}$'s can be written as a product of individual conditional PDFs, viz.

$$f_{\mathbf{W}|\mathbf{X_0},\mathbf{Y_0}}(w_1, \cdots, w_N|X_{0l}, Y_{0l}) = \prod_{k=1}^{N}\frac{1}{\Omega_k^2}\frac{w_k^m}{S_k^{m-1}}\exp(-\frac{(S_k^2+w_k^2)}{2\Omega_k^2})\ I_{m-1}\left(w_k\frac{S_k}{\Omega_k^2}\right), \quad l = 1, \cdots, m \quad (2.33)$$

where $\mathbf{W} = [\sqrt{R_1}, \cdots, \sqrt{R_N}]$, $\mathbf{X_0} = [X_{01}, \cdots, X_{0m}]$ and $\mathbf{Y_0} = [Y_{01}, \cdots, Y_{0m}]$.

From the laws of probability we know that [44]

$$f_{\mathbf{W}}(w_1, \cdots, w_N) = \int_{Y_{0l}}\int_{X_{0l}} f_{\mathbf{W},\mathbf{X_0},\mathbf{Y_0}}(w_1, \cdots, w_N, X_{0l}, Y_{0l})\ \ dX_{0l}dY_{0l}, l = 1, \cdots, m. \quad (2.34)$$

Also, we have

$$f_{\mathbf{W},\mathbf{X_0},\mathbf{Y_0}}(w_1,\cdots,w_N,X_{0l},Y_{0l}) = f_{\mathbf{W}|\mathbf{X_0},\mathbf{Y_0}}(w_1,\cdots,w_N|X_{0l},Y_{0l})\ \ f_{\mathbf{X_0},\mathbf{Y_0}}(X_{0l},Y_{0l}). \tag{2.35}$$

Then we can write the unconditional joint PDF as

$$f_{\mathbf{W}}(w_1,\cdots,w_N) = \iint\limits_{X_{0l},Y_{0l},l=1,\cdots,m} f_{\mathbf{W}|\mathbf{X_0},\mathbf{Y_0}}(w_1,\cdots,w_N|X_{0l},Y_{0l})\ \ f_{\mathbf{X_0},\mathbf{Y_0}}(X_{0l},Y_{0l})dX_{0l}dY_{0l},$$
$$l = 1,\cdots,m. \tag{2.36}$$

Since X_{0l}, Y_{0l} are independent and Gaussian distributed as $\mathcal{N}(0,\frac{1}{2})$, the joint PDF $f_{\mathbf{X_0},\mathbf{Y_0}}(X_{0l},Y_{0l})$ is given by

$$f_{\mathbf{X_0},\mathbf{Y_0}}(X_{0l},Y_{0l}) = \frac{1}{\pi^m}\exp(-\sum_{l=1}^{m} X_{0l}^2 + Y_{0l}^2). \tag{2.37}$$

Substituting (2.37) in (2.36), we get

$$f_{\mathbf{W}}(w_1,\cdots,w_N) = \iint\limits_{X_{0l},Y_{0l},l=1,\cdots,m} \prod_{k=1}^{N} \frac{1}{\Omega_k^2}\frac{w_k^m}{S_k^{m-1}}\exp(-\frac{(S_k^2+w_k^2)}{2\Omega_k^2})\ \ I_{m-1}\left(w_k\frac{S_k}{\Omega_k^2}\right)$$
$$\frac{1}{\pi^m}\exp(-\sum_{l=1}^{m} X_{0l}^2 + Y_{0l}^2)dX_{0l}dY_{0l}\ \ l = 1,\cdots,m. \tag{2.38}$$

We can simplify the $2m$-fold integral in (2.38) using a hyperspherical coordinate system transformation, where we substitute

$$\begin{aligned}
X_{01} &= Rcos(\phi_1)\\
Y_{01} &= Rsin(\phi_1)cos(\phi_2)\\
X_{02} &= Rsin(\phi_1)sin(\phi_2)cos(\phi_3)\\
&\vdots\\
X_{0m} &= Rsin(\phi_1)sin(\phi_2)\cdots cos(\phi_{2m})\\
Y_{0m} &= Rsin(\phi_1)sin(\phi_2)\cdots sin(\phi_{2m}).
\end{aligned} \tag{2.39}$$

Then we have $\sum_{l=1}^{m}(X_{0l}^2 + Y_{0l}^2) = R^2$ and $S_K^2 = \sigma_k^2\lambda_k^2R^2$. The Jacobian of the transformation can be found as

$$|J| = R^{2m-1}\ sin^{2m-2}(\phi_1)\ sin^{2m-3}(\phi_2)\ \cdots\ sin(\phi_{2m-2}) \tag{2.40}$$

and the joint PDF of the Nakagami-*m* RVs can be written as

$$f_{\mathbf{W}}(w_1, w_2, \cdots, w_N) = \int_{R=0}^{\infty}\int_{\phi_1=0}^{\pi}\int_{\phi_2=0}^{\pi}\cdots\int_{\phi_{2m-1}}^{2\pi} R^{2m-1}\ sin^{2m-2}(\phi_1)sin^{2m-3}(\phi_2)\cdots\ sin(\phi_{2m-2}) \frac{1}{\pi^m}\exp(R^2)\exp(-\sum_{k=1}^{N}\frac{S_k^2}{2\Omega_k^2})\prod_{k=1}^{N} I_{m-1}\left(w_k\frac{S_k}{\Omega_k^2}\right) \prod_{k=1}^{N}\frac{1}{S_k^{m-1}}\prod_{k=1}^{N}\frac{1}{\Omega_k^2}w_k^m\exp(-\frac{w_k^2}{2\Omega_k^2})d\phi_1 d\phi_2\cdots d\phi_{2m-1}dR. \quad (2.41)$$

To simplify the $2m$-fold integral in (2.41) to a single integral, we take the part of the integral which contains angles $\phi_1\cdots\phi_{2m}$

$$\int_{R=0}^{\infty}\int_{\phi_1=0}^{\pi}\int_{\phi_2=0}^{\pi}\cdots\int_{\phi_{2m-1}}^{2\pi} R^{2m-1}\ sin^{2m-2}(\phi_1)sin^{2m-3}(\phi_2)\cdots\ sin(\phi_{2m-2}) \frac{1}{\pi^m}\exp(-R^2)d\phi_1 d\phi_2\cdots d\phi_{2m-1}dR. \quad (2.42)$$

The problem of integrating out all the angles can be considered as deriving the envelope PDF of $2m$ independent Gaussian variables with zero mean and equal variance $\frac{1}{2}$. This PDF can be found as a central chi-distribution with $2m$ degrees of freedom [43]. Therefore, we can simplify the $2m$-fold integral in (2.42) to a single integral, namely

$$\int_0^{\infty} 2\frac{R^{2m-1}}{\Gamma(m)}\exp(-R^2)dR. \quad (2.43)$$

Then the joint PDF of Nakagami RVs can be written as

$$f_{\mathbf{W}}(w_1, \cdots, w_N) = \int_0^{\infty}\frac{t^{m-1}}{\Gamma(m)}e^{-t}\prod_{k=1}^{N}\frac{1}{(\sigma_k^2\lambda_k^2 t)^{\frac{m-1}{2}}} \frac{w_k^m}{\Omega_k^2}\ \exp\left(-\frac{w_k^2+\sigma_k^2\lambda_k^2 t}{2\Omega_k^2}\right) I_{m-1}\left(\frac{w_k\sqrt{\sigma_k^2\lambda_k^2}\sqrt{t}}{\Omega_k^2}\right)\ dt. \quad (2.44)$$

Eq. (2.44) can be rearranged and represented as a Laplace transform integral

$$f_{\mathbf{W}}(w_1, \cdots, w_N) = \left[\prod_{k=1}^{N}\frac{1}{(\sigma_k^2\lambda_k^2 t)^{\frac{m-1}{2}}}\frac{w_k^m}{\Omega_k^2}\exp(-\frac{w_k^2}{2\Omega_k^2})\right]\int_0^{\infty}\frac{t^{m-1}}{\Gamma(m)} \times\exp(-t(1+\sum_{k=1}^{N}\frac{\sigma_k^2\lambda_k^2}{2\Omega_k^2}))\prod_{k=1}^{N} I_{m-1}\left(\frac{w_k\sqrt{\sigma_k^2\lambda_k^2}\sqrt{t}}{\Omega_k^2}\right)\ dt \quad (2.45)$$

where the usual Laplace transform parameter s has the particular value $s = 1 + \sum_{k=1}^{N} \frac{\sigma_k^2 \lambda_k^2}{2\Omega_k^2}$.

Eq. (2.45) is a new single integral representation of a class of multivariate Nakagami-*m* PDF for integer order and identical fading severity parameter m. The solution is given in terms of well known mathematical functions available in common mathematical software packages such as MATLAB. No multiple nested infinite summations are required for the computation of the N-dimensional Nakagami-*m* PDF with the underlying complex Gaussian components having the correlation structure (2.6). A remarkable advantage of this representation is that the computational complexity is limited to a single integral computation for a N-dimensional PDF. Also as we show in the next section, the N-dimensional Nakagami-*m* CDF can be obtained directly without additional integration operations on the N-dimensional PDF.

We obtain a single integral representation of the multivariate Nakagami-*m* CDF using a similar approach by integrating (2.36) with respect to $w_1, w_2, \cdots, w_N$

$$F_{\mathbf{W}}(w_1, \cdots, w_N) = \int_{Y_{0l}} \int_{X_{0l}} F_{\mathbf{W}|\mathbf{X_0},\mathbf{Y_0}}(w_1, \cdots, w_N | X_{0l}, Y_{0l}) f_{\mathbf{X_0},\mathbf{Y_0}}(X_{0l}, Y_{0l}) \quad dX_{0l} dY_{0l} \quad l = 1, \cdots, m. \quad (2.46)$$

Since $w_1, \cdots, w_N$ conditioned on X_0 and Y_0 are independent, the joint conditional CDF of $w_1, \cdots, w_N$ can be written as

$$F_{\mathbf{W}|\mathbf{X_0},\mathbf{Y_0}}(w_1, \cdots, w_N | X_{0l}, Y_{0l}) = \prod_{k=1}^{N} F_{\sqrt{R_k}|\mathbf{X_0},\mathbf{Y_0}}(w_k | X_{0l}, Y_{0l}), \quad k = 1, \cdots, N \quad (2.47)$$

where $F_{\sqrt{R_k}|\mathbf{X_0},\mathbf{Y_0}}(w_k | X_{0l}, Y_{0l})$, $k = 1, \cdots, N$ is given by [43]

$$F_{\sqrt{R_k}|\mathbf{X_0},\mathbf{Y_0}}(w_k | X_{0l}, Y_{0l}) = \left[1 - Q_m\left(\frac{S_k}{\Omega_k}, \frac{w_k}{\Omega_k}\right)\right] \quad (2.48)$$

and $Q_m(a, b)$ is the m^{th} order generalized Marcum Q-function [43], which is available in common mathematical software packages such as MATLAB. S_k and Ω_k are as defined in Section (2.3.3).

Following the same methodology as in (2.39) and (2.43), we obtain the single integral representation of the multivariate Nakagami CDF, namely

$$F_{\mathbf{W}}(w_1, \cdots, w_N) = \int_0^{\infty} \frac{t^{m-1}}{\Gamma(m)} \exp(-t) \prod_{k=1}^{N} \left[1 - Q_m\left(\frac{\sqrt{t}\sqrt{\sigma_k^2 \lambda_k^2}}{\Omega_k}, \frac{w_k}{\Omega_k}\right)\right] dt. \quad (2.49)$$

Eq. (2.49) is a new representation for the CDF of a class of multivariate Nakagami-*m* distributions with identical and integer order fading severity parameters among the correlated RVs. Only a single integral computation is required to evaluate the N-dimensional Nakagami-*m* CDF with the correlation structure (2.6) among the corresponding complex Gaussian components. No multiple nested infinite summations are required for computation of the multivariate Nakagami-*m* CDF form given in (2.49). To the best of our knowledge, this single integral representation of the multivariate CDF is new. In [12], the CDF of the output SNR of a selection combiner was obtained for equally correlated Nakagami-*m* fading channels. Also reference [40] gives the output SNR CDF for a N-branch selection combiner operating in generalized correlated Nakagami-*m* fading, but the analysis is limited to positive values of λ_k. The results in this chapter are more general than the cases considered in [12] and [40]. We are unaware of any other study which provides simple forms for the multivariate Nakagami-*m* CDF with integer order fading severity parameter m. If we let $\sigma_1 = \sigma_2 = \sigma$, we get the case where the correlated Nakagami-*m* RVs are identically distributed.

2.4 Applications to Performance Analysis of Selection Diversity Combining

Here we use our new representations of multivariate Rayleigh, Rician and Nakagami-*m* distributions to analyze the performance of N-branch selection diversity combining (SC) in generalized correlated Rayleigh, Rician and Nakagami-*m* fading channels.

In SC, the combiner selects the branch with the largest instantaneous SNR. Then, the output SNR of the selection combiner is [47]

$$\gamma_{SC} = max(\gamma_1, \gamma_2, \cdots, \gamma_N). \tag{2.50}$$

The instantaneous SNR of the k^{th} branch can be given as

$$\gamma_k = \frac{|G_k|^2 E_s}{N_0} \tag{2.51}$$

where E_s is the transmitted symbol energy and N_0 is the additive white Gaussian noise (AWGN) power spectral density (PSD) at each branch. We assume identically distributed correlated fadings on the branches. Then, the average faded SNR, $\bar{\gamma_k}$, is given by

$$\bar{\gamma_k} = \bar{\gamma} = \frac{\mathbb{E}[|G_k|^2] E_s}{N_0}. \tag{2.52}$$

We denote $\frac{E_s}{N_0}$ by Γ, then $\bar{\gamma}$ equals Γ for the Rayleigh fading model assumed in (2.1). For the Rician fading case, the average SNR per branch is not equal across the branches. This is due to the correlation model (2.3) used in the analysis. Then $\bar{\gamma_k}$ for a Rician branch is equal to $(1 + K_k)\Gamma$.

2.4.1 Rayleigh fading

The CDF of the output SNR of the selection combiner for Rayleigh fading can be obtained as [47]

$$\begin{aligned} F_{\gamma_{SC}}(y) &= Pr(\gamma_1 < y, \gamma_2 < y, \cdots, \gamma_N < y) \\ &= \int_0^\infty \exp(-t) \prod_{k=1}^{N} \left[1 - Q\left(\sqrt{\frac{t\lambda_k^2}{\sigma_k^2}}, \sqrt{\frac{y}{\Gamma\sigma_k^2}} \right) \right] dt. \end{aligned} \tag{2.53}$$

We can calculate the outage probability of N-branch selection diversity in generalized correlated Rayleigh fading by replacing y by γ_{th} , the outage threshold SNR of the system. One has

$$\begin{aligned} Pr_{outage} &= Pr\left(|G_1| < \sqrt{\frac{\gamma_{th}}{\Gamma}}, |G_2| < \sqrt{\frac{\gamma_{th}}{\Gamma}}, \cdots, |G_N| < \sqrt{\frac{\gamma_{th}}{\Gamma}} \right) \\ &= \int_0^\infty \exp(-t) \prod_{k=1}^{N} \left[1 - Q\left(\sqrt{\frac{t\lambda_k^2}{\sigma_k^2}}, \sqrt{\frac{\gamma_{th}}{\Gamma\sigma_k^2}} \right) \right] dt. \end{aligned} \tag{2.54}$$

2.4.2 Rician fading

The CDF of the output SNR of the selection combiner for Rician fading can be found similarly as

$$\begin{aligned} F_{\gamma_{SC}}(y) &= Pr\left(|G_1| < \sqrt{\frac{y}{\Gamma}}, |G_2| < \sqrt{\frac{y}{\Gamma}}, \cdots, |G_N| < \sqrt{\frac{y}{\Gamma}} \right) \\ &= \int_0^\infty \exp(-t) \exp(-(m_1^2 + m_2^2)) I_0\left(2\sqrt{t}\sqrt{m_1^2 + m_2^2} \right) \\ &\qquad \times \prod_{k=1}^{N} \left[1 - Q\left(\sqrt{\frac{t\lambda_k^2}{\sigma_k^2}}, \sqrt{\frac{y}{\Gamma\sigma_k^2}} \right) \right] dt. \end{aligned} \tag{2.55}$$

Then we can similarly calculate the outage probability of N-branch selection combining in generalized correlated Rician fading by replacing y by γ_{th}, the outage threshold SNR of

the system, giving

$$\begin{aligned} Pr_{outage} &= Pr\left(|G_1| < \sqrt{\frac{\gamma_{th}}{\Gamma}}, |G_2| < \sqrt{\frac{\gamma_{th}}{\Gamma}}, \cdots, |G_N| < \sqrt{\frac{\gamma_{th}}{\Gamma}}\right) \\ &= \int_0^\infty \exp(-t)\exp(-(m_1^2+m_2^2))I_0\left(2\sqrt{t}\sqrt{m_1^2+m_2^2}\right) \\ &\qquad \times \prod_{k=1}^{N}\left[1 - Q\left(\sqrt{\frac{t\lambda_k^2}{\sigma_k^2}}, \sqrt{\frac{\gamma_{th}}{\Gamma\sigma_k^2}}\right)\right] dt. \end{aligned} \tag{2.56}$$

In [12], N-branch selection diversity combining was analyzed for the more restrictive case of equicorrelated Rayleigh and Rician fading using a single integral representation of the multivariate CDF, while in [40], a similar result for correlated Rayleigh fading was obtained, but which admits only positive values of λ_k. As an additional minor point, we are not aware of any literature dealing with N-branch selection combining in correlated Rician fading channels with a generalized correlation model which admits negative as well as positive correlations among the underlying complex Gaussian RVs. Examples of wireless channels with negative correlation can be found in [48].

2.4.3 Nakagami-*m* fading

The CDF of the output SNR of the selection combiner can be obtained as [47]

$$\begin{aligned} F_{\gamma_{SC}}(y) &= Pr(\gamma_1 < y, \gamma_2 < y, \cdots, \gamma_N < y) \\ &= Pr(R_1 < \frac{y}{\Gamma}, R_2 < \frac{y}{\Gamma}, \cdots, R_N < \frac{y}{\Gamma}) \\ &= Pr\left(\sqrt{R_1} < \sqrt{\frac{y}{\Gamma}}, \sqrt{R_2} < \sqrt{\frac{y}{\Gamma}}, \cdots, \sqrt{R_N} < \sqrt{\frac{y}{\Gamma}}\right) \\ &= \int_{t=0}^{\infty} \frac{t^{m-1}}{\Gamma(m)}\exp(-t)\prod_{k=1}^{N}\left[1 - Q_m\left(\frac{\sqrt{t}\sqrt{\sigma_k^2\lambda_k^2}}{\Omega_k}, \sqrt{\frac{y}{\Gamma\Omega_k^2}}\right)\right] dt. \end{aligned} \tag{2.57}$$

The outage probability of N-branch selection diversity operating in correlated Nakagami-*m* fading can now be calculated by substituting γ_{th} , the outage threshold SNR of the system, in (2.57). One has

$$\begin{aligned} &Pr_{outage} \\ &= Pr\left(\sqrt{R_1} < \sqrt{\frac{\gamma_{th}}{\Gamma}}, \sqrt{R_2} < \sqrt{\frac{\gamma_{th}}{\Gamma}}, \cdots, \sqrt{R_N} < \sqrt{\frac{\gamma_{th}}{\Gamma}}\right) \\ &= \int_{t=0}^{\infty} \frac{t^{m-1}}{\Gamma(m)}\exp(-t)\prod_{k=1}^{N}\left[1 - Q_m\left(\sqrt{\frac{t\sigma_k^2\lambda_k^2}{\Omega_k^2}}, \sqrt{\frac{\gamma_{th}}{\Gamma\Omega_k^2}}\right)\right] dt \end{aligned} \tag{2.58}$$

as the final solution.

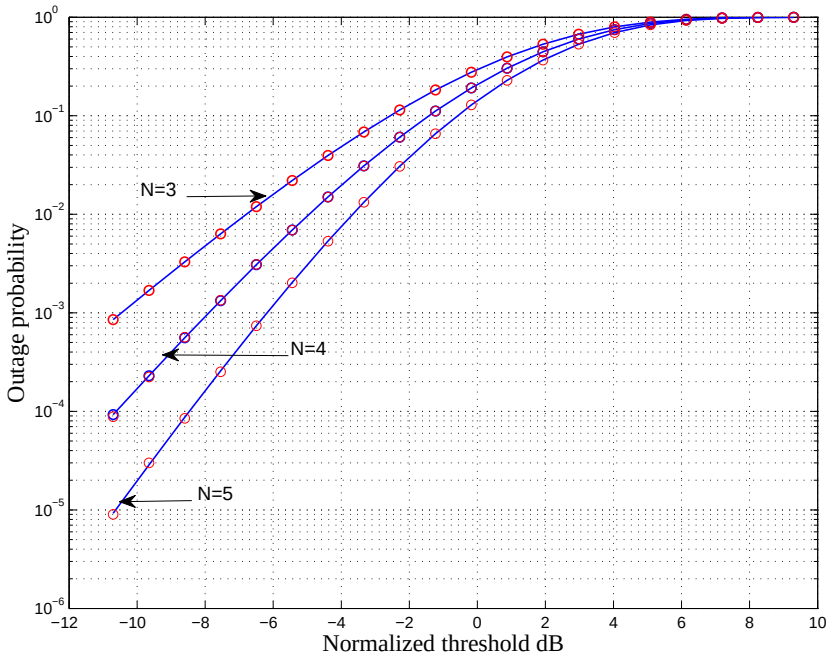

Figure 2.1. The outage probability in Rayleigh fading for N=3, 4 and 5 branches.

2.5 Numerical Results and Discussion

In this section, we present some numerical examples and simulation results for the outage probability of selection diversity combining operating in correlated Rayleigh, Rician and Nakagami-*m* fading. We use $\overrightarrow{\rho} = [\lambda_1, \lambda_2, \cdots, \lambda_N]$ to denote the set of λ_k values used in the theoretical and simulation results.

Fig.2.1 shows the outage performance of N-branch selection combining in correlated Rayleigh fading for $N = 3, 4$ and 5. For $N = 3$, we have used $\overrightarrow{\rho} = [0.8, -0.4, 0.7]$, for $N = 4$, $\overrightarrow{\rho} = [0.8, -0.4, 0.7, -0.6]$, and $\overrightarrow{\rho} = [0.8, -0.4, 0.7, -0.6, 0.5]$ for $N = 5$. The normalized threshold $\gamma^*$is calculated as γ_{th}/Γ. One can see that the theoretical results are in excellent agreement with simulation results. As in the case with independent fading, the outage performance improves with an increasing number of branches but the marginal benefit diminishes with an increasing number of branches.

Fig. 2.2 shows the outage performance of N-branch selection combining in correlated Rician fading for $N = 3, 4$ and 5. We use the same respective sets of $\overrightarrow{\rho}$ as for Rayleigh fading for $N = 3, 4$ and 5, and we set $m_1, m_2 = 2$ in our theoretical computations and simulations. The normalized threshold $\gamma^*$is calculated as γ_{th}/Γ. Note that in the Rician

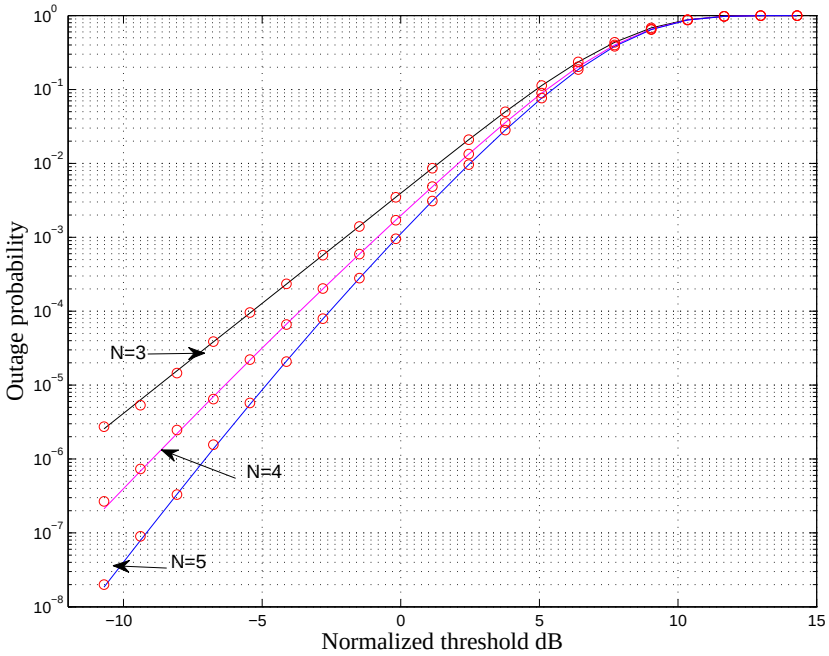

Figure 2.2. The outage probability in Rician fading for N=3, 4 and 5 branches.

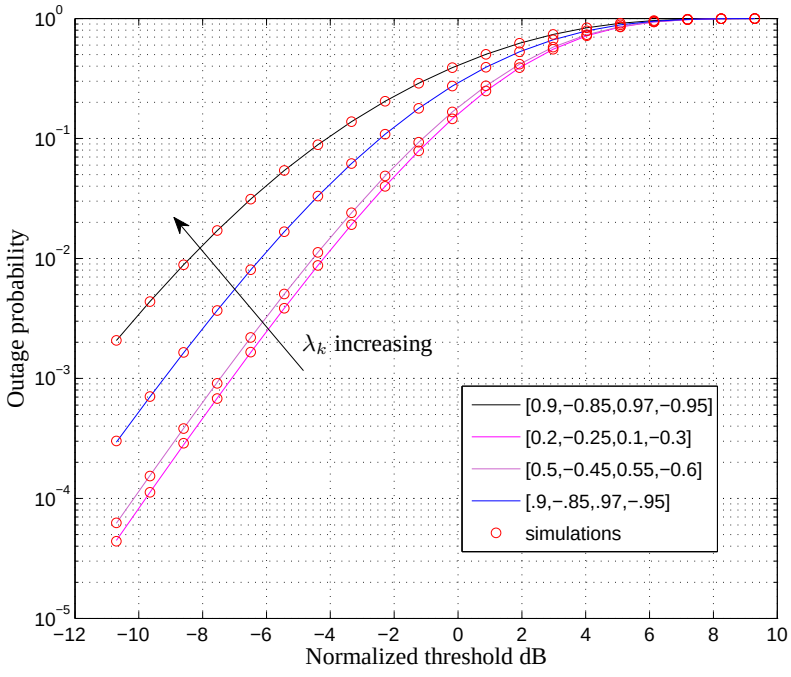

Figure 2.3. The effect of correlation on the outage probability for 4-branch selection combining in correlated Rayleigh fading.

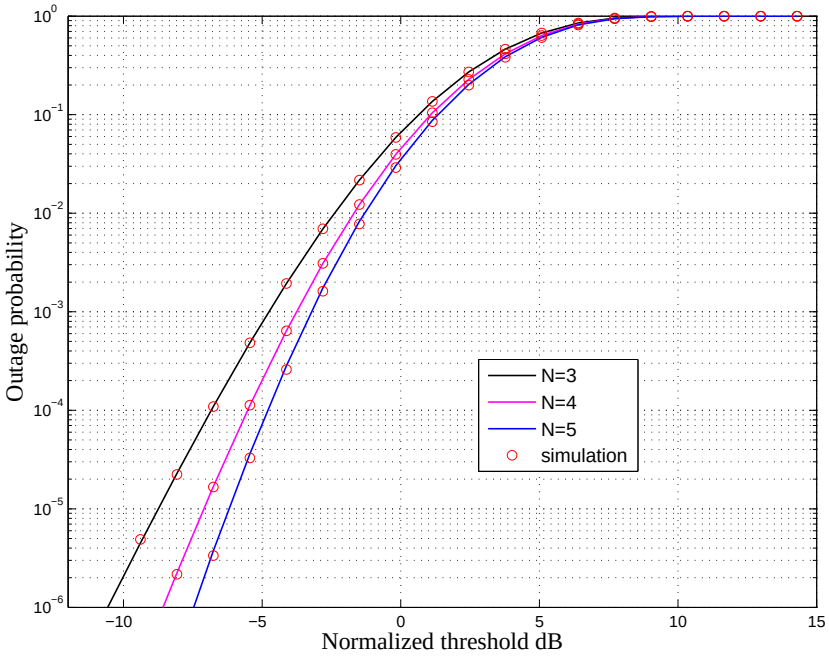

Figure 2.4. The outage probability for N-branch selection combining in correlated Nakagami-*m* fading for N=3, 4 and 5 with m=2.

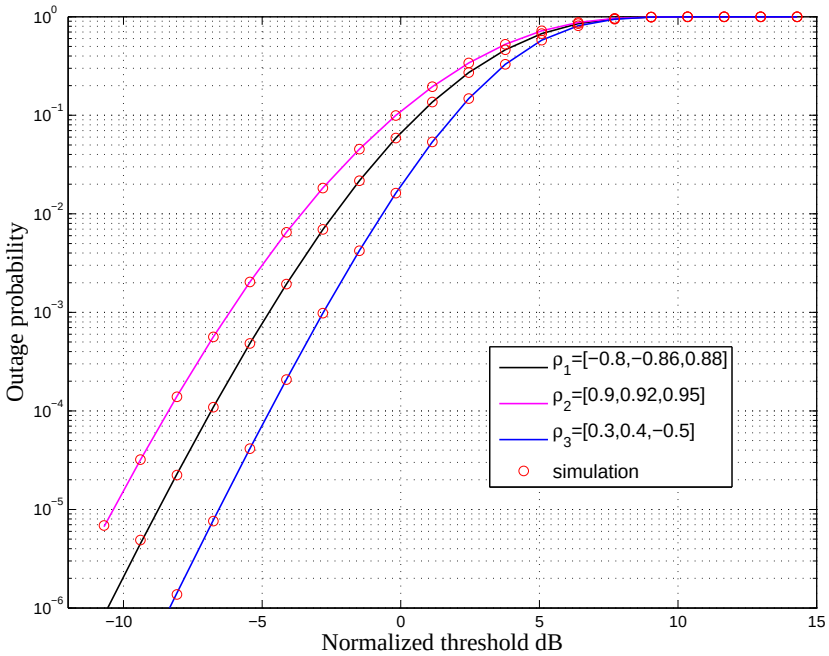

Figure 2.5. The effect of the magnitudes of the λ_k values on the outage probability for 3-branch selection diversity in Nakagami-*m* fading with m=2.

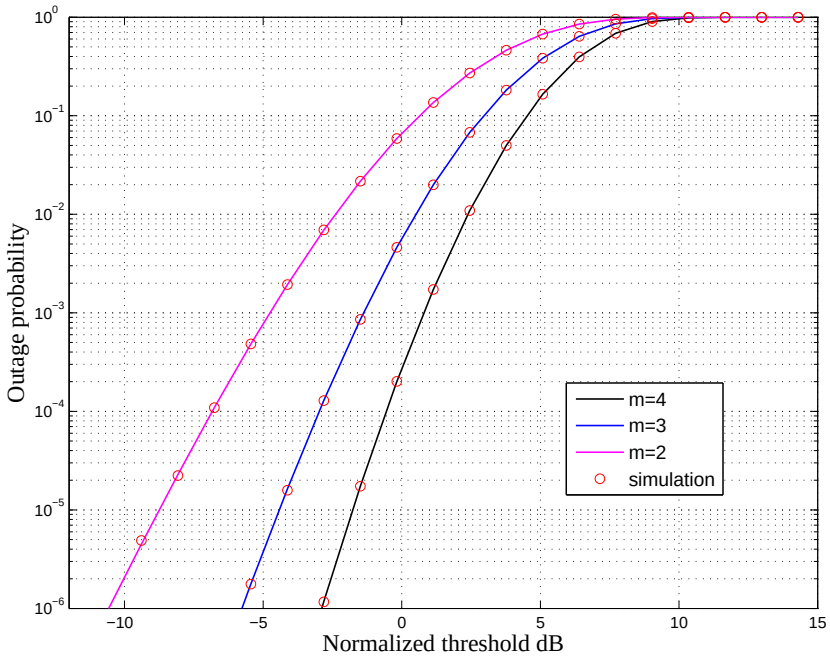

Figure 2.6. The outage probability for 3-branch selection diversity in correlated Nakagami-*m* fading for $m = 2,\ 3$ and 4.

case, the branch fadings are not identically distributed. One can see the excellent agreement between the theoretical results and simulation results in all cases.

Fig. 2.3 shows the effect of the values of λ_k on the outage performance in correlated Rayleigh fading. We have used sets of λ_k with values ranging from low to high. Since correlation between G_k and G_j is given as $\lambda_k\lambda_j$, by changing the values of λ_k, we change the magnitude of the correlation between the G_ks. We observe that the outage performance deteriorates as the magnitudes of the λ_k values increase, as expected.

Note that we have used both negative and positive values of cross-correlations between the G_ks in our examples. The results obtained with the new PDF and CDF representations derived in this chapter are more general than the results in [12] and [40], which do not allow negative values of correlation in the underlying Gaussian RVs.

Fig. 2.4 shows the outage probability of N-branch selection diversity in correlated Nakagami-*m* fading for N=3, 4 and 5. The λ_k values used in theoretical computations and simulation are denoted as $\rho = [\lambda_1, \lambda_2, \cdots, \lambda_N]$. We have assumed $m = 3$ for the results in Fig. 2.4. We have used $\rho = [0.8, -0.86, 0.88]$ for $N = 3$, $\rho = [0.8, -0.86, 0.88, 0.9]$ for $N = 4$ and $\rho = [0.8, -0.86, 0.88, 0.9, 0.92]$ for $N = 5$ in the theoretical calculations

and simulations. For simplicity, we used $\sigma_k = \sigma = 1, k = 1, \cdots, N$ in our results. The normalized threshold γ^* is calculated as γ_{th}/Γ.

Fig. 2.5 shows the effect of the magnitude of the λ_k values on the outage probability of 3-branch selection combining operating in generalized correlated Nakagami-*m* fading. We used $m = 2$ in our simulations and theoretical calculations. The power correlation between R_k and R_j is given by $\lambda_k^2\lambda_j^2$. Therefore by increasing values of λ_k, we increase the power correlation across branches. We can observe that the outage performance deteriorates as the magnitudes of the λ_k values increase.

Fig. 2.6 shows the outage probability of 3-branch selection diversity operating in generalized correlated Nakagami-*m* fading for different values of fading severity parameter m. We used λ_k values $\rho = [0.8, -0.86, 0.88]$ for the results in Fig. 2.6. The outage performance improves as the fading severity parameter value increases from 2 to 4. One can see the excellent agreement between the theoretical and simulation results in all the cases considered.

2.6 Summary

In this chapter, we presented novel single integral representations for the PDF and the CDF of a class of multivariate Rayleigh, Rician and Nakagami-*m* distributions with a generalized correlation structure. An important feature of this solutions is that the numerical evaluation complexity is limited to a single integral computation for an arbitrary number of correlated RVs. Another benefit of the new solution is that the CDF is computed directly, and with a single integration, not requiring multiple (N for N-dimensional distributions) integrations to calculate the CDF from the PDF. Also we used the new forms of the CDF to evaluate the outage probability of N-branch selection combining in correlated Rayleigh, Rician and Nakagami-*m* fadings. Simulation results were used to verify the accuracy of the theoretical results.

Chapter 3

New Representations for the Multivariate Non-Central Chi-Square Distribution With Constant Correlation

3.1 Introduction

In this chapter,[1] motivated by the limited availability of mathematical representations for the multivariate non-central χ^2 distributions, we derive new single integral representations for the PDF and CDF of the multivariate non-central χ^2 distribution when the underlying Gaussian RVs follow the equal correlation model. The advantage of the new representation is that the N-dimensional distribution can be computed by evaluating a single integral. The new expressions for the PDF and CDF are given in-terms of well known mathematical functions which are readily available in common mathematical software packages such as MATLAB. The basic idea for the methodology used in this study is found in [41].

The remainder of this chapter is organized as follows. In Section 3.2, we present the model used to generate correlated RVs using a special linear combination of independent Gaussian RVs. Detailed derivation of the multivariate non-central χ^2 PDF and CDF is presented in Section 3.3. Section 3.4 presents an application of the new CDF representation to a multiple antenna system with receiver antenna selection operating in correlated Rician fading channels. Some numerical examples and simulation results are presented in Section 3.5.

[1] A version of this chapter has been submitted to the *IEEE Transactions on Communications*.

3.2 Representation of Equicorrelated RVs

We use uppercase bold letters to denote matrices and lowercase bold letters for vectors. We use $(\cdot)^T$ and $(\cdot)^H$ to denote the transpose and the Hermitian transpose of a matrix, respectively.

Using the method described in [41, eq.(8.1.6)] we define a Gaussian RV as

$$G_{kl} = (\sqrt{1-\lambda^2}X_{kl} + \lambda X_{0l}) + m_{0l} \qquad k = 1, \cdots, N, \;\; l = 1, \cdots, m \tag{3.1}$$

where $\lambda \in (-1, 1) \setminus \{0\}$ and $X_{kl}(k = 0, 1, \cdots, N \;\; l = 1, \cdots, m)$ are independent and $\mathcal{N}(0, \frac{1}{2})$. Then for any $k, j \in \{1, \cdots, N\}$, $l, n \in \{1, \cdots, m\}$, $\mathbb{E}[X_{kl}X_{jn}] = \delta_{kj}\delta_{ln}$, where $\delta_{kk} = 1$ and $\delta_{kj} = 0$ for $k \neq j$. The cross-correlation coefficient between any G_{kl} and G_{jn} $(k \neq j)$ is given by

$$\begin{aligned} \rho_{kl,jn} &= \frac{\mathbb{E}[G_{kl}G_{jn}^*] - \mathbb{E}[G_{kl}]\mathbb{E}[G_{jn}^*]}{\sqrt{\text{Var}[G_{kl}] \;\; \text{Var}[G_{jn}]}} \\ &= \begin{cases} \lambda^2 & (k \neq j \text{ and } l = n) \\ 0 & (l \neq n). \end{cases} \end{aligned} \tag{3.2}$$

Denote R_k as the summation of squared values of G_{kl} for $l = 1, \cdots, m$, then

$$R_k = \sum_{l=1}^{m} G_{kl}^2. \tag{3.3}$$

Note that $R_k(k = 1, \cdots, N)$ is a summation of squares of m independent Gaussian RVs with non-zero means and identical variances. Then it is evident that $R_k(k = 1, \cdots, N)$ is a set of correlated non-central χ^2 distributed RVs with m degrees of freedom and non-centrality parameter ξ, where ξ is equal to $\sum_{l=1}^{m} m_{0l}^2$. The component Gaussian RVs follow the equal correlation model.

3.3 Derivation of PDF and CDF of Multivariate Non-Central χ^2 Distribution

In this section, we present the derivation of the PDF and CDF of the multivariate non-central χ^2 distribution with equal correlation among the component Gaussian RVs. We introduce a new RV, $U_{0l} = X_{0l} + \frac{m_{0l}}{\lambda}$. Define another new RV T such that

$$T = \sum_{l=1}^{m} U_{0l}^2. \tag{3.4}$$

We identify that T is non-central χ^2 distributed with m degrees of freedom and non-centrality parameter $S^2 = \sum_{l=1}^{m} \left(\frac{m_{0l}}{\lambda}\right)^2$. The PDF of T is given by [43]

$$f_T(t) = \left(\frac{t}{S^2}\right)^{\frac{m-2}{4}} \exp(-(S^2+t)) I_{\frac{m}{2}-1}\left(2S\sqrt{t}\right). \tag{3.5}$$

Now assume the values of RVs U_{0l} are fixed at u_{0l} for $l = 1, \cdots, m$. Then the value of T also becomes fixed at t. Now we consider the conditional RVs G_{kl}s. Note that the RVs G_{kl}s conditioned on RVs U_{0l}s have equal variances $(1-\lambda^2)/2$ and means λu_{0l}. We identify that the RVs R_ks conditioned on U_{0l} are also non-central χ^2 distributed with m degrees of freedom and non-centrality parameter $C^2 = \lambda^2 \sum_{l=1}^{m} u_{0l}^2 = \lambda^2 t$. We can write the conditional PDF of R_k as [43]

$$f_{R_k|\mathbf{U_0}}(r_k|U_{01}, \cdots, U_{0m}) = \frac{1}{2\Omega_k^2}\left(\frac{r_k}{\lambda^2 t}\right)^{\frac{m-2}{4}} \exp\left(-\frac{(\lambda^2 t + r_k)}{2\Omega_k^2}\right) \; I_{\frac{m}{2}-1}\left(\sqrt{r_k}\frac{\sqrt{\lambda^2 t}}{\Omega_k^2}\right) \tag{3.6}$$

where $\Omega_k^2 = (1-\lambda^2)/2$ and $\mathbf{U_0} = [U_{01}, \cdots, U_{0m}]$.

One can compute the conditional cross-correlation coefficient between G_{kl} and G_{jn} using

$$\rho^c_{kl,jn} = \frac{\mathbb{E}[G_{kl}G_{jn}|X_0, Y_0] - \mathbb{E}[G_{kl}|X_0, Y_0]\mathbb{E}[G_{jn}|X_0, Y_0]}{\sqrt{\mathbb{E}[(G_{kl} - \mathbb{E}[G_{kl}])^2|X_0, Y_0]\,\mathbb{E}[(G_{jn} - \mathbb{E}[G_{jn}])^2|X_0, Y_0]}} = 0. \tag{3.7}$$

The G_{kl}s are conditionally uncorrelated. Since they are jointly Gaussian distributed, they are conditionally independent. Since the components G_{kl} are independent once conditioned on U_{0l}, the resulting R_k's become conditionally independent for $k = 1, \cdots, N$. Then the conditional joint PDF of the resulting R_k's can be written as a product of the individual PDFs,

$$f_{\mathbf{R}|T}(r_1, r_2, \cdots, r_N|t) = \prod_{k=1}^{N} \frac{1}{2\Omega_k^2}\left(\frac{r_k}{\lambda^2 t}\right)^{\frac{m-2}{4}} \exp\left(-\frac{\lambda^2 t + r_k}{2\Omega_k^2}\right) I_{\frac{m}{2}-1}\left(\sqrt{r_k}\frac{\sqrt{\lambda^2 t}}{\Omega_k^2}\right), \tag{3.8}$$

where $\mathbf{R} = [R_1, \cdots, R_N]$.

From the basic laws of probability we have [44]

$$f_{\mathbf{R}}(r_1, r_2, r_3, \cdots, r_N) = \int_0^\infty f_{\mathbf{R},T}(r_1, r_2, \cdots, r_N, t) \;\; dt. \tag{3.9}$$

Also we have

$$f_{\mathbf{R},T}(r_1, r_2, \cdots, r_N, t) = f_{\mathbf{R}|T}(r_1, r_2, \cdots, r_N|t) \;\; f_T(t). \tag{3.10}$$

Then we can write the unconditional joint PDF as

$$f_{\mathbf{R}}(r_1, r_2, r_3, \cdots, r_N) = \int_0^\infty f_{\mathbf{R}|T}(r_1, r_2, \cdots, r_N|t) \;\; f_T(t) \;\; dt. \tag{3.11}$$

Substituting (3.5) and (3.8) into eq. (3.11), we get

$$f_{\mathbf{R}}(r_1, r_2, \cdots, r_N) = \int_0^\infty \left(\frac{t}{S^2}\right)^{\frac{m-2}{4}} \exp\left(-(S^2+t)\right) I_{\frac{m}{2}-1}\left(2S\sqrt{y}\right) \prod_{k=1}^{N} \frac{1}{2\Omega_k^2}\left(\frac{r_k}{\lambda^2 t}\right)^{\frac{m-2}{4}} \exp\left(-\frac{\lambda^2 t + r_k}{2\Omega_k^2}\right) I_{\frac{m}{2}-1}\left(\sqrt{r_k}\frac{\sqrt{\lambda^2 t}}{\Omega_k^2}\right) dt. \tag{3.12}$$

Eq. (3.12) is the new single integral representation for the multivariate non-central χ^2 distribution with the component Gaussian RVs having an equal correlation structure. The solution is given in terms of well known mathematical functions available in common mathematical software packages such as MATLAB. No multiple nested infinite summations are required for the computation of the N-dimensional PDF. The computational burden is limited to a numerical evaluation of a single integral for a N-dimensional distribution.

The multivariate CDF for the non-central chi-square distribution can be obtained using a similar methodology.

$$F_{\mathbf{R}}(r_1, \cdots, r_N) = \int \cdots \int F_{\mathbf{R}|\mathbf{U_0}}(r_1, \cdots, r_N|U_{01}, \cdots, U_{0m}) \;\; f_{\mathbf{U_0}}(U_{01}, \cdots, U_{0m}) \;\; dU_{01} \cdots dU_{0m}. \tag{3.13}$$

Since the RVs R_ks are conditionally independent on $U_{01}, \cdots, U_{0m}$, the joint conditional CDF can be written as the product of individual conditional CDFs as

$$F_{\mathbf{R}|\mathbf{U_0}}(r_1, r_2, \cdots, r_N|U_{01}, \cdots, U_{0m}) = \prod_{k=1}^{N} F_{R_k|\mathbf{U_0}}(r_k|U_{01}, \cdots, U_{0m}) \tag{3.14}$$

where $F_{R_k|\mathbf{U_0}}(r_k|U_{01}, \cdots, U_{0m})$ can be obtained using [43]

$$F_{R_k|\mathbf{U_0}}(r_k|U_{01}, \cdots, U_{0m}) = \sum_{j=0}^{\infty} e^{\frac{\Delta^2}{2}} \frac{(\Delta^2/2)^j}{j!} \frac{\gamma(j+(m/2), (1-\lambda^2)r_k/2)}{\Gamma(j+(m/2))} \tag{3.15}$$

where $\Delta^2 = \frac{2C^2}{1-\lambda^2}$, $j = \sqrt{-1}$, $\gamma(a, b)$ is the lower incomplete gamma function [49] and $\Gamma(\cdot)$ is the gamma function [49] . For even values of m, we can write this CDF in terms of generalized Marcum-Q function [43], namely

$$F_{R_k|\mathbf{U_0}}(r_k|U_{01}, \cdots, U_{0m}) = 1 - Q_{m/2}\left(\frac{C}{\Omega_k}, \frac{\sqrt{r_k}}{\Omega_k}\right). \tag{3.16}$$

Using the same approach used for the multivariate PDF derivation, we derive the single-integral representation for the CDF of the multivariate non-central chi-square distribution as

$$F_{\mathbf{R}}(r_1, r_2, \cdots, r_N) = \int_0^\infty \left(\frac{t}{S^2}\right)^{\frac{m-2}{4}} \exp(-(S^2+t)) I_{\frac{m}{2}-1}\left(2S\sqrt{y}\right) \prod_{k=1}^{N} \sum_{j=0}^{\infty} e^{\frac{\Delta^2}{2}} \frac{(\Delta^2/2)^j}{j!} \frac{\gamma(j+(m/2), (1-\lambda^2) r_k/2)}{\Gamma(j+(m/2))} dt \quad (3.17)$$

and for the special case of even m,

$$F_{\mathbf{R}}(r_1, \cdots, r_N) = \int_0^\infty \left(\frac{t}{S^2}\right)^{\frac{m-2}{4}} \exp(-(S^2+t)) I_{\frac{m}{2}-1}\left(2S\sqrt{y}\right) \prod_{k=1}^{N} \left[1 - Q_{\frac{m}{2}}\left(\frac{\sqrt{\lambda^2 t}}{\Omega_k}, \frac{\sqrt{r_k}}{\Omega_k}\right)\right] dt. \quad (3.18)$$

Eqs. (3.17) and (3.18) are the new single-integral representations for a multivariate non-central χ^2 distribution with the component Gaussian RVs having the equal correlation structure (3.2). Contrary to the representations given in [13], [33], [34], the computational time required does not grow exponentially with the dimensionality of the distribution. Note that the infinite series in (3.17) can be computed easily with the function NCX2CDF available in MATLAB.

Using the single integral representation of the multivariate PDF, the joint CHF of $\mathbf{R}$ can be found in single integral form as

$$\Psi_{\mathbf{R}}(\omega_1, \cdots, \omega_N) = \int_0^\infty \left(\frac{t}{S^2}\right)^{\frac{m-2}{4}} \exp\left(-(S^2+t)\right) I_{\frac{m}{2}-1}\left(2S\sqrt{t}\right) \prod_{k=0}^{N} \frac{1}{(1-j\omega_k\Omega_k^2)^{1/2}} \exp\left(\frac{j\omega_k S^2}{1-j2\omega_k\Omega_k^2}\right) dt. \quad (3.19)$$

3.4 Applications of the New Representations

The new representation derived for the CDF of the multivariate non-central χ^2 distribution can be used to evaluate the outage probability of a single-user MIMO system with receiver antenna selection. MIMO systems, which marked a remarkable advancement in wireless communication technologies, were introduced to provide both diversity and capacity enhancement in a wireless system, subject to a fundamental tradeoff. The implementation of MIMO technology requires the availability of multiple radio frequency (RF) chains in

wireless devices, leading to higher implementation complexity. In order to achieve the benefit of having multiple antennas while maintaining a reasonable system complexity, several antenna selection schemes have been proposed for MIMO systems [50], [51].

Independent fading channels are assumed in the majority of studies that deal with the performance of antenna selection in MIMO systems. However, in practical scenarios, the fading experienced by different antenna elements can be correlated. The performance of MIMO systems with antenna selection, operating in Rayleigh fading channels in the presence of fading correlation was investigated in [52], [53]. The exponential correlation model is used in [52] for the case when the number of receiver antennas is greater than 3. In this section, we examine the performance of a single-user MIMO system which employs receiver antenna selection, operating in correlated Rician fading channels. We consider a MIMO system model with N_t transmitter antennas and N_r receiver antennas. The received signal after the matched filter can be written in vector form as

$$\mathbf{y} = \mathbf{H}\mathbf{x} + \mathbf{n} \tag{3.20}$$

where $\mathbf{n}$ denotes the N_r-dimensional noise vector and the N_t-dimensional independent and identically distributed (i.i.d.) signal vector is denoted as $\mathbf{x}$. The $N_r \times N_t$-dimensional channel matrix $\mathbf{H}$ is modeled using

$$h_{ij} = \left(\sqrt{1-\lambda^2}X_{ij} + \lambda X_{0j} + m_1\right) + \sqrt{-1}\left(\sqrt{1-\lambda^2}Y_{ij} + \lambda Y_{0j} + m_2\right) \tag{3.21}$$

where h_{ij} denotes the channel coefficient from the j^{th} transmit antenna to the i^{th} receive antenna, $\lambda \in (-1,1) \setminus \{0\}$ and $X_{ij}, Y_{ij} (i = 0, 1, \cdots, N_r \;\; j = 1, \cdots, N_t)$ are independent and $\mathcal{N}(0, \frac{1}{2})$. The RV h_{ij} is $N_C((m_1 + \sqrt{-1}m_2), 1)$, and $|h_{ij}|$ is Rician distributed with Rician factor $K = (m_1^2 + m_2^2)$ and mean-square value $\mathbb{E}[|h_{ij}|^2] = 1 + K$. The cross-correlation coefficient between any h_{kl} and h_{jn} $(k \neq j)$ is given by

$$\begin{aligned} \rho_{kl,jn} &= \frac{\mathbb{E}[h_{kl}h_{jn}^*] - \mathbb{E}[h_{kl}]\mathbb{E}[h_{jn}^*]}{\sqrt{\text{Var}[h_{kl}] \;\; \text{Var}[h_{jn}]}} \\ &= \begin{cases} \lambda^2 & (k \neq j \text{ and } l = n) \\ 0 & (l \neq n). \end{cases} \end{aligned} \tag{3.22}$$

Therefore, the model given in (3.21) can represent correlated Rician RVs with the underlying complex Gaussian RVs following the equal correlation model (3.22).

The channel matrix $\mathbf{H}$ can be written as

$$\mathbf{H} = [\mathbf{h_1}, \cdots, \mathbf{h_{N_t}}] = [\mathbf{p_1}, \cdots, \mathbf{p_{N_r}}]^{\mathbf{T}} \tag{3.23}$$

where $\mathbf{h_i}$ and $\mathbf{p_j}$ denote the columns and rows of $\mathbf{H}$ respectively. From the correlation model (3.22) we identify that the $\mathbf{h}_\mathrm{i}$ $(i = 1, \cdots, N_t)$ are mutually independent and the elements of each $\mathbf{h_i}$ are equally correlated. The equal correlation model [10], [12], [54] is considered to be valid for a closely placed set of antennas and may be used as a worst case performance benchmark [12]. We assume perfect channel state information (CSI) only at the receiver. The transmitter uses equal power allocation among the all transmitter antennas. The instantaneous capacity of the MIMO system can be obtained as

$$C_{inst} = \log_2 \det \left(\mathbf{I}_{\mathrm{N_r}} + \frac{\rho}{\mathrm{N_t}} \mathbf{H}\mathbf{H}^{\mathrm{H}} \right) \tag{3.24}$$

where ρ is the average unfaded SNR which is equal to $\frac{E}{\sigma_n^2}$, $E = \mathrm{x}^{\mathrm{H}}\mathrm{x}$ and σ_n^2 is the variance of the noise.

Similar to the system model used in [52], we assume that only one receiver antenna which maximizes the instantaneous capacity is selected at the receiver. Let C_i denote the instantaneous capacity if the i^{th} receiver antenna is selected. Then the achievable capacity with the antenna selection scheme can be written as [52]

$$C_{\mathrm{sys}} = \max \{C_1, C_2, \cdots, C_{N_r}\} \tag{3.25}$$

where C_i is given as

$$C_i = \log_2 \left(1 + \frac{\rho}{N_t} W_i \right) \tag{3.26}$$

and where $W_i = \mathbf{p}_i^H \mathbf{p}_i = \sum_{k=1}^{N_t} |h_{ij}|^2$. We identify that W_i is non-central chi-square distributed with $2N_t$ degrees of freedom. Note that C_i is maximized when W_i is maximized. Then we define $Z = \max \{W_1, W_2, \cdots, W_{N_r}\}$, and the achievable capacity with antenna selection can be written as

$$C_{\mathrm{sys}} = \log_2 \left(1 + \frac{\rho}{N_t} Z \right). \tag{3.27}$$

3.4.1 Outage probability of the system

Following the same outage probability definition used in [52], we consider an outage event to occur when the instantaneous capacity of the system falls below a threshold information

rate. Then the system outage probability can be calculated as

$$\begin{aligned} Pr_{\text{outage}} &= Pr\left\{C_{\text{sys}} \leq C_{\text{th}}\right\} \\ &= Pr\left\{\log_2\left(1+\frac{\rho}{N_t}Z\right) \leq C_{\text{th}}\right\} \\ &= Pr\left\{Z \leq \frac{N_t(2^{C_{\text{th}}}-1)}{\rho}\right\} \\ &= F_Z\left(\frac{N_t(2^{C_{\text{th}}}-1)}{\rho}\right). \end{aligned} \tag{3.28}$$

Also we have

$$\begin{aligned} F_Z(z) &= Pr\left\{Z \leq z\right\} \\ &= Pr\left\{W_1 \leq z, \cdots, W_{N_r} \leq z\right\} \\ &= F_{\{W_1,\cdots,W_{N_r}\}}\left(z, \cdots, z\right). \end{aligned} \tag{3.29}$$

The single integral expression for outage can be given as

$$\begin{aligned} &Pr\left\{C_{\text{sys}} \leq C_{\text{th}}\right\} \\ &= F_{\{W_1,\cdots,W_{N_r}\}}\left(\frac{N_t(2^{C_{\text{th}}}-1)}{\rho}, \cdots, \frac{N_t(2^{C_{\text{th}}}-1)}{\rho}\right) \\ &= \int_0^\infty \frac{t^{\frac{2N_t-2}{4}}}{S_1^{N_t-1}} e^{-(t+S_1^2)} I_{N_t-1}(S_1\sqrt{t}) \left[1 - Q_{N_t}\left(\sqrt{\frac{2\lambda^2 t}{1-\lambda^2}}, \sqrt{\frac{\frac{2N_t(2^{C_{\text{th}}}-1)}{\rho}}{1-\lambda^2}}\right)\right]^{N_r} dt \end{aligned} \tag{3.30}$$

where $S_1^2 = N_t(m_1^2+m_2^2)/\lambda^2$. To the best of our knowledge, this result is novel. Compared to previous results, we are unaware of outage analysis on MIMO receiver antenna selection in correlated Rician fading that do not place restrictions on the dimensions of the system.

3.5 Numerical Results

In Fig. 3.1, the outage probability is plotted for the case when $N_t = 3$ and $N_r = 3, 4, 5$ and 6 with $\lambda = 0.7$, and Rice factor $K = 3$ dB. A threshold information rate of 2 bits/s/Hz is assumed for the numerical and simulation results. It can be observed that the outage probability improves with additional receiver antennas, as expected. However, the marginal benefit with each additional receiver antenna is decreasing. For example, when N_r increases from 3 to 4, we obtain a SNR gain of 1.2 dB while the gain is 0.6 dB for the case when N_r increase from 5 to 6. Fig. 3.1 also shows the outages for uncorrelated antennas. Observe

that the marginal benefit of an additional receiver antenna is smaller in the correlated case. Fig. 3.2 shows the outage probability variation with the number of transmitter antennas when $N_r = 3$, $\lambda = 0.7$ and the Rice factor $K = 3$ dB. We observe SNR gains of 1.7 dB when N_t changes from 3 to 4 and 1.1 dB when N_t changes from 4 to 5 at an outage probability of 10^{-6}. The new representation of the CDF permits accurate comparison of the correlated system with the uncorrelated antenna system. The outage probability behavior for the case of $N_t, N_r = 3$ with different λ values is plotted in Fig. 3.3. The SNR loss due to fading correlation can be clearly quantified from Fig. 3.3. Fig 3.4 shows the system outage probability for different K values. A SNR gain of 7.5 dB can be observed for the correlated system when K varies from 1 dB to 7 dB with outage probability of 10^{-6}, demonstrating clearly the benefit of increased power in the line-of-sight component. The single integral expressions are evaluated using numerical integration in MATLAB, while one may use other numerical integration techniques to evaluate the single integral to a desired accuracy.

3.6 Summary

Novel single-integral representations were derived for the PDF and the CDF of a multivariate non-central χ^2 distribution with the underlying Gaussian RVs following the equal correlation model. The solutions were given in terms of mathematical functions which are available in common mathematical software packages such as MATLAB. An important feature of these solutions is that the computational burden remains at the level of a single integral computation for a N-dimensional distribution. We used the new form of the multivariate CDF to numerically evaluate the outage probability of MIMO systems with receiver antenna selection, operating in equally correlated Rician fading channels. Finally numerical examples and simulation results were given to demonstrate the accuracy of the new solutions.

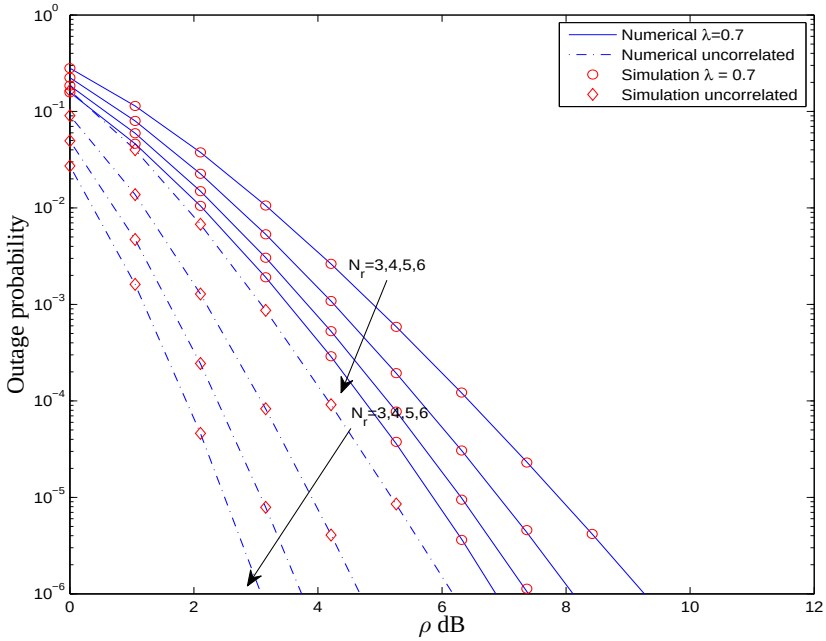

Figure 3.1. The outage probability for $N_t = 3$ with different values of N_r with $\lambda = 0.7$ and $K = 3$ dB.

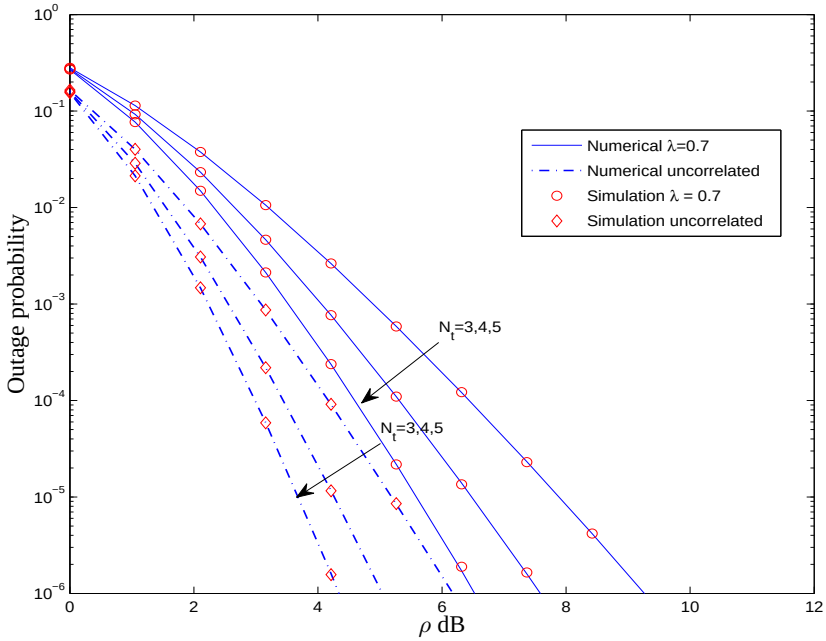

Figure 3.2. The outage probability for $N_r = 3$ with different values of N_t with $\lambda = 0.7$ and $K = 3$ dB.

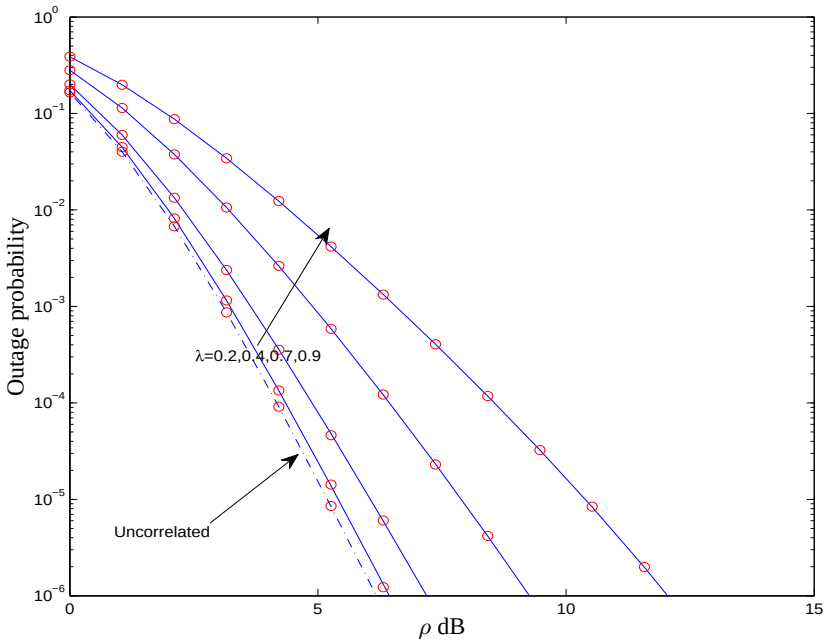

Figure 3.3. The outage probability for $N_t = 3$ and $N_r = 3$ for different values of λ.

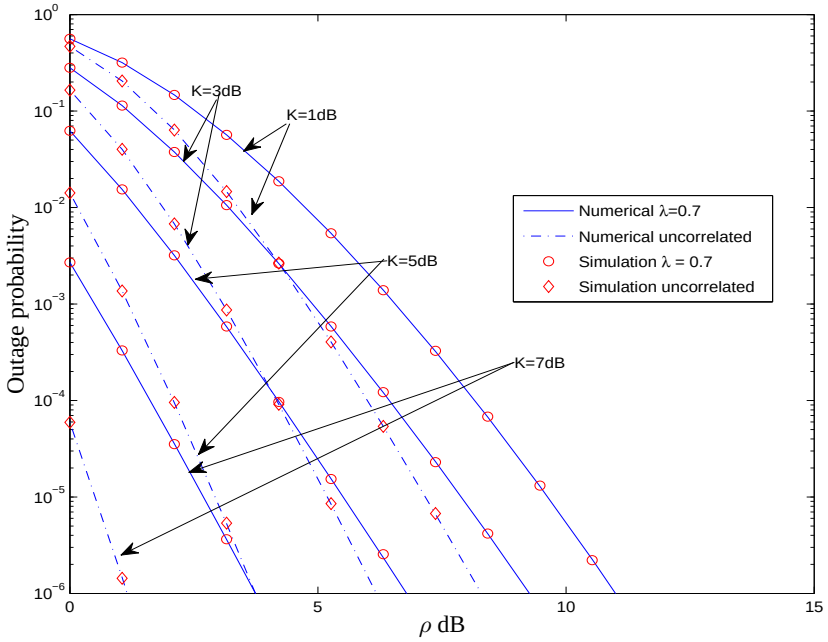

Figure 3.4. The outage probability for $N_r = N_t = 3$ at $\lambda = 0.7$ with different K values.

Chapter 4

New Representations for the Multivariate Weibull Distribution With Constant Correlation

4.1 Introduction

In this chapter[1], we derive single integral representations for the PDF and CDF of the joint multivariate Weibull distribution with constant correlation. We use the new representations to evaluate the performance of a selection diversity system operating in equally correlated Weibull fading channels. The advantage of this approach is that the complexity of the numerical evaluation of the distributions does not grow exponentially with the number of dimensions of the distribution, as is the case for some previously known results. The new representations are given in terms of well known mathematical functions which can be easily and rapidly evaluated with commonly available mathematical software packages such as MATLAB. Thus the performance measures of a selection diversity scheme can be computed conveniently. References [12], [40] used this approach for performance evaluation of correlated Rayleigh, Rician and Nakagami-*m* fading channels. The basic idea for this approach is found in [41]. Furthermore, we show how to use our new representations to execute moment analysis of the output SNR of EGC diversity operating in equally correlated Weibull fading channels. Previously, only the average output SNR (first moment) of EGC in correlated Weibull fading has been studied [56].

The remainder of this chapter is organized as follows. In Section 4.2, we present the model used to generate equally correlated Weibull RVs from independent Gaussian RVs.

[1]This chapter will be presented in part at the IEEE Global Communications Conference (GLOBECOM) 2010 [55].

The approach used to derive the multivariate Weibull PDF and CDF is presented in Section 4.3. In Section 4.4, we use the new representation of multivariate Weibull CDF for performance evaluation of a selection diversity system operating in correlated Weibull fading. Section 4.5 presents the output SNR moment analysis of EGC in equally correlated Weibull fading using the new multivariate PDF representation. Numerical examples and simulation results are presented in Section 4.6.

4.2 Representation of Correlated Weibull RVs

The Weibull fading model has several definitions. In [6], it was shown that Weibull distributed RVs can be generated by a power transformation on Rayleigh distributed RVs. Therefore we denote a set of correlated Rayleigh distributed RVs using the approach given in [41, eq. (8.1.6)],

$$G_k = \sigma_k(\sqrt{1-\lambda^2}X_k + \lambda X_0) + i\sigma_k(\sqrt{1-\lambda^2}Y_k + \lambda Y_0) \tag{4.1}$$

where $i = \sqrt{-1}$, $\lambda \in (-1,1) \setminus \{0\}$ and $X_k, Y_k (k = 0, \cdots, L)$ are independent and $\mathcal{N}(0, \frac{1}{2})$. Then for any $k, j \in \{0, \cdots, L\}$, $\mathbb{E}[X_k Y_j] = 0$, and $\mathbb{E}[X_k X_j] = \mathbb{E}[Y_k Y_j] = \frac{1}{2}\delta_{kj}$ where $\delta_{kk} = 1$ and $\delta_{kj} = 0$ for $k \neq j$. Then G_k is a zero-mean complex Gaussian distribution with $N_c(0, \sigma_k^2)$, and $|G_k|$ is Rayleigh distributed with mean square value $\mathbb{E}[|G_k|^2] = \sigma_k^2$. It can be shown that the correlation coefficient between any G_k, G_j for $k \neq j$ is given by

$$\varrho_{k,j} = \frac{\mathbb{E}[G_k G_j^*] - \mathbb{E}[G_k]\mathbb{E}[G_j^*]}{\sqrt{\mathbb{E}[|G_k|^2]\mathbb{E}[|G_j|^2]}} = \lambda^2. \tag{4.2}$$

According to [6, eq. (1)], we denote the complex envelope W_k of the Weibull fading model as

$$W_k = (\sigma_k(\sqrt{1-\lambda^2}X_k + \lambda X_0) + i\sigma_k(\sqrt{1-\lambda^2}Y_k + \lambda Y_0))^{\frac{2}{\beta}} \tag{4.3}$$

where the Weibull power parameter $\beta > 0$.

Let $Z_k = |W_k|$. Then we can write Z_k as a power transformation of a Rayleigh distributed RV $|G_k|$, namely

$$Z_k = |G_k|^{\frac{2}{\beta}} \tag{4.4}$$

where $|G_k|$ is determined by (4.1) with the correlation structure (4.2). The corresponding correlations between the resulting Weibull RVs can be calculated using [6, eq. (15)]. Using this power transformation on correlated Rayleigh RVs, we can obtain correlated Weibull

RVs with identical power parameter β and the m^{th} moment given by

$$\mathbb{E}[Z_k^m] = \sigma_k^{2m/\beta}\Gamma\left(1+\frac{m}{\beta}\right). \tag{4.5}$$

By changing the value of β, we can obtain RVs with other distributions such as the Rayleigh and the negative exponential.

4.3 Derivation of the PDF and CDF of the Multivariate Weibull Distribution

In this section, we present the derivation of the new representations for multivariate Weibull distributions with constant correlation. As the first step, we condition the RVs G_ks on the RVs X_0 and Y_0. The PDF and CDF of $|G_k|$ conditioned on X_0 and Y_0, can be written as

$$f_{|G_k|}(r_k|X_0,Y_0) = \frac{r_k}{\Omega_k^2}\exp\left(-\frac{(r_k^2+\mu_k^2)}{2\Omega_k^2}\right) I_0\left(\frac{r_k\mu_k}{\Omega_k^2}\right) \tag{4.6a}$$

$$F_{|G_k|}(r_k|X_0,Y_0) = \left[1-Q\left(\frac{\mu_k}{\Omega_k},\frac{r_k}{\Omega_k}\right)\right] \tag{4.6b}$$

$$\mu_k^2 = \mu_x^2+\mu_y^2 \tag{4.6c}$$

$$\mu_x = \sigma_k\lambda X_0 \tag{4.6d}$$

$$\mu_y = \sigma_k\lambda Y_0 \tag{4.6e}$$

$$\Omega_k^2 = \sigma_k^2\left(\frac{1-\lambda^2}{2}\right), \quad k=1,\cdots,L. \tag{4.6f}$$

One can compute the conditional cross-correlation coefficient between G_k and G_j using

$$\varrho_{kj}^c = \frac{\mathbb{E}[G_kG_j^*|X_0,Y_0]-\mathbb{E}[G_k|X_0,Y_0]\mathbb{E}[G_j^*|X_0,Y_0]}{\sqrt{\mathbb{E}[|G_k-\mathbb{E}[G_k]|^2|X_0,Y_0]\,\mathbb{E}[|G_j-\mathbb{E}[G_j]|^2|X_0,Y_0]}} = 0. \tag{4.7}$$

The conditional PDF and CDF of the Z_k's can be written as

$$f_{Z_k}(z_k|X_0,Y_0) = \frac{\beta z_k^{\beta-1}}{2\Omega_k^2}\exp\left(-\frac{(z_k^\beta+\mu_k^2)}{2\Omega_k^2}\right) I_0\left(\frac{z_k^{\frac{\beta}{2}}\mu_k}{\Omega_k^2}\right) \tag{4.8a}$$

$$F_{Z_k}(z_k|X_0,Y_0) = \left[1-Q\left(\frac{\mu_k}{\Omega_k},\frac{z_k^{\frac{\beta}{2}}}{\Omega_k}\right)\right]. \tag{4.8b}$$

The RVs G_k's become uncorrelated when they are conditioned on the RVs X_0 and Y_0. Since the G_ks are jointly Gaussian distributed, they are conditionally independent. Therefore, the resulting RVs, the $|G_k|$s are independent. Since we obtain Z_k using a power transformation

on $|G_k|$, the resulting Z_ks also become conditionally independent. Then the conditional joint PDF of the Z_ks can be written as the product of the individual conditional PDFs, namely

$$f_{\mathbf{Z}|X_0,Y_0}(z_1, z_2, \cdots, z_L|X_0, Y_0) = \prod_{k=1}^{L} f_{Z_k}(z_k|X_0, Y_0) \tag{4.9}$$

where $\mathbf{Z} = [Z_1, Z_2, \cdots, Z_L]$. From the laws of probability, we know that [44]

$$f_{\mathbf{Z}}(z_1, \cdots, z_L) = \int_{Y_0} \int_{X_0} f_{\mathbf{Z},X_0,Y_0}(z_1, z_2, \cdots, z_L, X_0, Y_0) \quad dX_0 dY_0. \tag{4.10}$$

Also we have

$$f_{\mathbf{Z},X_0,Y_0}(z_1, \cdots, z_L, X_0, Y_0) = f_{\mathbf{Z}|X_0,Y_0}(z_1, z_2, \cdots, z_L|X_0, Y_0) \;\; f_{X_0,Y_0}(X_0, Y_0). \tag{4.11}$$

Then we can write the unconditional joint PDF as

$$f_{\mathbf{Z}}(z_1, \cdots, z_L) = \int_{Y_0} \int_{X_0} f_{\mathbf{Z}|X_0,Y_0}(z_1, z_2, \cdots, z_L|X_0, Y_0) \;\; f_{X_0,Y_0}(X_0, Y_0) \quad dX_0 dY_0. \tag{4.12}$$

Since X_0, Y_0 are independent and $\mathcal{N}(0, \frac{1}{2})$, the joint PDF is given by

$$f_{X_0,Y_0}(X_0, Y_0) = \frac{1}{\pi} \exp(-(X_0^2 + Y_0^2)). \tag{4.13}$$

Then we can write the joint unconditional PDF of the correlated Weibull RVs as

$$f_{\mathbf{Z}}(z_1, \cdots, z_L) = \int_{Y_0} \int_{X_0} \prod_{k=1}^{L} f_{Z_k|X_0,Y_0}(z_k|X_0, Y_0) \;\; \frac{1}{\pi} \exp(-(X_0^2 + Y_0^2)) \quad dX_0 dY_0. \tag{4.14}$$

Substituting (4.8) in (4.14), and after some straightforward manipulations, we can simplify the double integral in (4.14) to obtain a single integral representation for the PDF of the multivariate Weibull distribution as

$$f_{\mathbf{Z}}(z_1, \cdots, z_L) = \int_{t=0}^{\infty} \exp(-t) \prod_{k=1}^{L} \frac{\beta z_k^{\beta-1}}{2\Omega_k^2} \exp\left(-\frac{z_k^{\beta} + \sigma_k^2 \lambda^2 t}{2\Omega_k^2}\right) I_0\left(\frac{z_k^{\frac{\beta}{2}} \sqrt{t\sigma_k^2 \lambda^2}}{\Omega_k^2}\right) \quad dt. \tag{4.15}$$

Eq. (4.15) is the new single integral representation for the PDF of a Gaussian class multivariate Weibull distribution with constant correlation. The L-dimensional PDF can be

computed by numerically evaluating the single integral representation. An interesting observation regarding this representation compared to previously available forms [6, eq. (29)], is that the numerical implementation and evaluation complexity does not increase exponentially with the number of dimensions in the distribution.

For the special case of $L = 2$, eq. (4.15) can be solved in closed-form using [57, eq. (3.15.17.1)] to obtain

$$f_{Z_1,Z_2}(z_1,z_2) = \frac{\beta_1\beta_2 z_1^{\beta_1-1} z_2^{\beta_2-1}}{\sigma_1^2\sigma_2^2(1-\lambda^4)} \exp\left[-\frac{1}{1-\lambda^4}\left(\frac{z_1^{\beta_1}}{\sigma_1^2}+\frac{z_2^{\beta_2}}{\sigma_2^2}\right)\right] I_0\left(\frac{2\sqrt{\lambda^4} z_1^{\beta_1/2} z_2^{\beta_2/2}}{\sigma_1\sigma_2(1-\lambda^4)}\right) \quad (4.16)$$

which was previously given in [6, eq. (11)].

In order to obtain a new representation for the multivariate Weibull CDF, we integrate (4.12) with respect to variables $z_1, z_2, \cdots, z_L$, and we get

$$F_{\mathbf{Z}}(z_1,\cdots,z_L) = \int_{Y_0}\int_{X_0} F_{\mathbf{Z}|X_0,Y_0}(z_1,z_2,\cdots,z_L|X_0,Y_0)\ f_{X_0,Y_0}(X_0,Y_0)\ dX_0dY_0 \quad (4.17)$$

where $F_{\mathbf{Z}|X_0,Y_0}(z_1,z_2,\cdots,z_L|X_0,Y_0)$ is given by

$$F_{\mathbf{Z}|X_0,Y_0}(z_1,z_2,\cdots,z_L|X_0,Y_0) = \prod_{k=1}^{L} F_{Z_k|X_0,Y_0}(z_k|X_0,Y_0) \quad (4.18)$$

and where $F_{Z_k|X_0,Y_0}(z_k|X_0,Y_0)$ is defined in (4.8).

Substituting (4.8) and (4.13) in (4.17), we get

$$F_{\mathbf{Z}}(z_1,\cdots,z_L) = \int\int \prod_{k=1}^{L}\left[1-Q\left(\frac{\mu_k}{\Omega_k},\frac{z_k^{\frac{\beta}{2}}}{\Omega_k}\right)\right]\frac{1}{\pi}\exp(-(X_0^2+Y_0^2))dX_0dY_0. \quad (4.19)$$

Using the same manipulations we used for the multivariate PDF derivation, we get the single integral form for the multivariate Weibull CDF with equally correlated RVs as

$$F_{\mathbf{Z}}(z_1,\cdots,z_L) = \int_{t=0}^{\infty} e^{-t}\prod_{k=1}^{L}\left[1-Q\left(\frac{\sqrt{t}\sqrt{\sigma_k^2\lambda^2}}{\Omega_k},\frac{z_k^{\frac{\beta}{2}}}{\Omega_k}\right)\right]dt. \quad (4.20)$$

Eq. (4.20) is the new representation for the CDF of a Gaussian class multivariate Weibull distribution with constant correlation. The L-dimensional CDF can be computed by numerically evaluating the single integral representation. Note that once again the numerical implementation and evaluation complexity does not grow exponentially with the number of dimensions in the distribution.

Also note that if we consider that only the underlying Rayleigh (or complex Gaussian) RVs are equally correlated (but not the resulting Weibull RVs as in [36]), we can modify our new representations to include non-identical values of power parameter $\beta_k > 0$ by replacing β with $\beta_k, k = 1, \cdots, L$. Therefore, the results presented in this chapter are more general than the results given in [6].

4.4 Performance of a L-branch Selection Diversity Combiner Operating in Equally Correlated Weibull Fading Channels

In this section, we use the new representations of the multivariate Weibull CDF for performance evaluation of a selection diversity combiner operating in equally correlated Weibull fading channels. We show that the outage probability for a L-branch selection combiner can be obtained in single integral form using the new representation of the multivariate Weibull CDF. Also, the average symbol error rate (SER) of some coherent and non-coherent modulation schemes can be evaluated in double integral form.

4.4.1 CDF of the output SNR

The complex baseband representation of the received signal at the k^{th} branch is given by

$$r_k = z_k x + n_k \tag{4.21}$$

where x is the data symbol with energy E_s, $z_k, k = 1, \cdots, \mathrm{L}$ are the channel gains modeled as Weibull RVs and $n_k, k = 1, \cdots, \mathrm{L}$ are zero-mean Gaussian noise samples with variance N_0, assumed to be equal across all the branches. The instantaneous SNR of the k^{th} branch can be given as

$$\gamma_k = \frac{z_k^2 E_s}{N_0}. \tag{4.22}$$

The average faded SNR, $\bar{\gamma}_k$, is given by

$$\bar{\gamma}_k = \frac{\mathbb{E}[z_k^2] E_s}{N_0}. \tag{4.23}$$

We denote $\frac{E_s}{N_0}$ by E. Then, $\bar{\gamma}_k = E\sigma_k^{4/\beta_k}\Gamma\left(1 + \frac{2}{\beta_k}\right)$. Using the interesting property that the n^{th} power of a Weibull distributed RV with parameters (β, σ^2) is another Weibull RV with parameters $(\beta/n, \sigma^2)$ [6], the joint CDF of the branch SNRs can be obtained by replacing β_k with $\beta_k/2$ and σ_k^2 with $(a_k\bar{\gamma}_k)^{\beta_k/2}$, where $a_k = 1/\Gamma(1 + \frac{2}{\beta_k})$.

The joint CDF of the branch SNRs is given by

$$F_{\boldsymbol{\gamma}}(\gamma_1, \cdots, \gamma_L) = \int_{t=0}^{\infty} e^{-t} \prod_{k=1}^{L} \left[1 - Q\left(\sqrt{\frac{2t\lambda^2}{1-\lambda^2}}, \sqrt{\frac{2\Upsilon_k^{\frac{\beta_k}{2}}}{1-\lambda^2}} \right) \right] dt \tag{4.24}$$

where $\Upsilon_k = \left(\frac{\gamma_k}{a_k \bar{\gamma_k}} \right)$ and $\boldsymbol{\gamma} = [\gamma_1, \gamma_2, \cdots, \gamma_L]$. The SC selects the branch with the largest instantaneous SNR. The output SNR of SC is given by

$$\gamma_{SC} = \max(\gamma_1, \gamma_2, \cdots, \gamma_L). \tag{4.25}$$

The CDF of γ_{SC} can be expressed as

$$\begin{aligned} F_{\gamma_{SC}}(y) &= Pr(\gamma_1 < y, \gamma_2 < y, \cdots, \gamma_L < y) \\ &= F_{\boldsymbol{\gamma}}(y, y, \cdots, y). \end{aligned} \tag{4.26}$$

Then one has

$$F_{\gamma_{SC}}(y) = \int_{0}^{\infty} e^{-t} \prod_{k=1}^{L} \left[1 - Q\left(\sqrt{\frac{2t\lambda^2}{1-\lambda^2}}, \sqrt{\frac{2\Upsilon_k^{\frac{\beta_k}{2}}}{1-\lambda^2}} \right) \right] dt. \tag{4.27}$$

For the case of identically distributed fading with $\sigma_k = \sigma$, and $\beta_k = \beta, k = 1, \cdots, L$, the CDF can be written as

$$F_{\gamma_{SC}}(y) = \int_{0}^{\infty} e^{-t} \left[1 - Q\left(\sqrt{\frac{2t\lambda^2}{1-\lambda^2}}, \sqrt{\frac{2\Upsilon^{\frac{\beta}{2}}}{1-\lambda^2}} \right) \right]^L dt. \tag{4.28}$$

4.4.2 PDF of output SNR

A single integral expression for the PDF of the output SNR of the selection combiner can be obtained by differentiating eqs. (4.27) and (4.28), namely

$$\begin{aligned} f_{\gamma_{SC}}(y) = \int_{t=0}^{\infty} e^{-t} \sum_{k=1}^{L} \frac{\beta_k y^{\beta_k/2-1}}{2(a\bar{\gamma_k})^{\beta_k/2}} \exp\left(-\frac{(\frac{y}{a_k\bar{\gamma_k}})^{\frac{\beta_k}{2}}}{(1-\lambda^2)} \right) I_0\left(2\sqrt{\frac{t\lambda^2}{1-\lambda^2}\left(\frac{y}{a_k\bar{\gamma_k}}\right)^{\frac{\beta_k}{2}}} \right) \\ \prod_{j\neq k} \left[1 - Q\left(\sqrt{2t\lambda^2}, \sqrt{\frac{2}{1-\lambda^2}\left(\frac{y}{a_j\bar{\gamma_j}}\right)^{\frac{\beta_j}{2}}} \right) \right] dt \end{aligned} \tag{4.29}$$

and

$$f_{\gamma_{SC}}(y) = \int_{t=0}^{\infty} e^{-t} \frac{L\beta y^{\beta/2-1}}{2(a\bar{\gamma})^{\beta/2}} \left[1 - Q\left(\sqrt{2t\lambda^2}, \sqrt{\frac{2}{1-\lambda^2}\left(\frac{y}{a\bar{\gamma}}\right)^{\frac{\beta}{2}}}\right)\right]^{L-1} \exp\left(-\frac{(\frac{y}{a\bar{\gamma}})^{\frac{\beta}{2}}}{(1-\lambda^2)}\right) I_0\left(2\sqrt{\frac{t\lambda^2}{1-\lambda^2}\left(\frac{y}{a\bar{\gamma}}\right)^{\frac{\beta}{2}}}\right) dt \quad (4.30)$$

for the identically distributed case.

The MGFs for each case can be obtained in double integral form by taking the Laplace transform of the PDFs in (4.29), (4.30).

4.4.3 Performance measures for selection combining

The expressions we derived for the PDF, CDF and MGF of the output SNR can be used to evaluate some performance measures of a selection diversity combiner operating in correlated Weibull fading.

Average Symbol Error Rate

The average symbol error rate (SER) of some coherent and noncoherent modulation formats can be evaluated by averaging the conditional error probability (CEP) $P(e|\gamma)$ over the PDF of the output SNR. Therefore, we can evaluate the average SER using

$$\bar{P_e} = \int_0^{\infty} P(e|\gamma) f_{\gamma_{SC}}(\gamma) d\gamma. \quad (4.31)$$

Alternatively, one can use the CDF approach which is given in [12, eq. (32)] to evaluate error rates using the CDF of the output SNR. In both cases, the average SER for a large family of modulations can be computed by numerically evaluating a double integral for an arbitrary number of diversity branches. The expressions for the CEP of some coherent and noncoherent modulation formats are given in [43].

Outage Proability

The outage probability of the system is found using

$$P_{\text{Outage}} = Pr(0 \leq \gamma_{SC} \leq \gamma_{th}) = F_{\gamma_{SC}}(\gamma_{th}) \quad (4.32)$$

where γ_{th} is the threshold SNR of the system. The system outage can be evaluated using a single integral computation for an arbitrary number of diversity branches.

Average SNR

Average SNR is another output quality measure of a wireless communication system. The average output SNR for the selection combiner can be evaluated using

$$\begin{aligned}\bar{\gamma}_{SC} &= \mathbb{E}[\gamma_{SC}] \\ &= -\frac{dM_{\gamma_{SC}}(s)}{ds}\Big|_{s=0} \\ &= \int_0^\infty \int_0^\infty e^{-t} \sum_{k=1}^{L} \frac{\beta_k y^{\beta_k/2}}{2(a\bar{\gamma}_k)^{\beta_k/2}} \exp\left(-\frac{(\frac{y}{a_k\bar{\gamma}_k})^{\frac{\beta_k}{2}}}{(1-\lambda^2)}\right) I_0\left(2\sqrt{\frac{t\lambda^2}{1-\lambda^2}\left(\frac{y}{a_k\bar{\gamma}_k}\right)^{\frac{\beta_k}{2}}}\right) \\ &\prod_{j\neq k}\left[1 - Q\left(\sqrt{2t\lambda^2}, \sqrt{\frac{2}{1-\lambda^2}\left(\frac{y}{a_j\bar{\gamma}_j}\right)^{\frac{\beta_j}{2}}}\right)\right] dtdy.\end{aligned} \tag{4.33}$$

More generally, the n^{th} moment of the SC output SNR can be found using

$$m_n = -\frac{d^n M_{\gamma_{SC}}(s)}{ds^n}\Big|_{s=0}. \tag{4.34}$$

4.5 Output SNR Moment Analysis of a L-branch Equal Gain Combiner

The new representation derived for the multivariate Weibull PDF can be used to examine the performance of an equal gain receiver operating in equally correlated Weibull fading channels. We mainly focus on deriving expressions for the moments of the EGC output SNR. The output SNR moments can be used to gain insight into the system performance in correlated fading channels. Furthermore, they can be used to evaluate performance measures such as average SER and outage probability using the standard approximation procedures developed in previous studies [58]. Reference [58] analyzed the output SNR moments for an equal gain receiver operating in equally correlated Rayleigh, Rician and Nakagami-*m* fading channels.

We use the same signal model given in (4.21) for our analysis. In EGC, the received signals are cophased and added to obtain the combiner output. The instantaneous SNR for the EGC output can be written as [47]

$$\gamma_{\text{egc}} = \frac{(z_1 + z_2 + \cdots + z_L)^2 E_s}{LN_0}. \tag{4.35}$$

With the aid of the multinomial identity, the moments of the combiner output SNR can be evaluated as [59]

$$m_n = \mathbb{E}[\gamma_{\text{egc}}^n] = \mathbb{E}\left[\left(\frac{(z_1+z_2+\cdots+z_L)^2 E_s}{LN_0}\right)^n\right] = \frac{(2n)!E_s^n}{(LN_0)^n}\sum_{\substack{n_1,\cdots,n_L=0\\ n_1+\cdots+n_L=2n}}^{2n}\left(\frac{\mathbb{E}[z_1^{n_1}\cdots z_L^{n_L}]}{\prod_{j=1}^{L} n_j!}\right). \tag{4.36}$$

In order to evaluate the moments of the combiner output SNR, we need to evaluate the joint moments of channel gains $\mathbb{E}(z_1^{n_1},\cdots,z_n^{n_L})$. The joint moments can be evaluated using the new representation of the multivariate Weibull PDF obtained in (4.15) as,

$$\mathbb{E}[z_1^{n_1},\cdots,z_n^{n_L}] = \underbrace{\int\int\cdots\int}_{\text{L-fold}}(z_1^{n_1},\cdots,z_n^{n_L}) f_{\mathbf{Z}}(z_1,z_2,\cdots,z_L)\, dz_1 dz_2\cdots dz_L. \tag{4.37}$$

Note that the L-fold integral in (4.37) is separable, and can be written as a product, namely

$$\mathbb{E}[z_1^{n_1},\cdots,z_n^{n_L}] = \int_0^\infty \exp(-t)\prod_{k=1}^{L}\int_0^\infty z_k^{n_k}\frac{\beta z_k^{\beta-1}}{2\Omega_k^2}\exp\left(-\frac{z_k^\beta+\sigma_k^2\lambda^2 t}{2\Omega_k^2}\right) I_0\left(\frac{z_k^{\frac{\beta}{2}}\sqrt{t\sigma_k^2\lambda^2}}{\Omega_k^2}\right) dz_k dt. \tag{4.38}$$

We denote the integral inside the product as $J(k)$ such that

$$J(k) = \int_0^\infty z_k^{n_k}\frac{\beta z_k^{\beta-1}}{2\Omega_k^2}\exp\left(-\frac{z_k^\beta+\sigma_k^2\lambda^2 t}{2\Omega_k^2}\right) I_0\left(\frac{z_k^{\frac{\beta}{2}}\sqrt{t\sigma_k^2\lambda^2}}{\Omega_k^2}\right) dz_k. \tag{4.39}$$

Using [60, eqs. (6.643.2) and (9.220.2)] , (4.39) can be solved in closed-form as

$$J(k) = \Gamma(1+\frac{n_k}{\beta})(2\Omega^2)^{\frac{n_k}{\beta}}\ {}_1F_1\left(-\frac{n_k}{\beta};1;-\frac{\lambda^2 t}{1-\lambda^2}\right) \tag{4.40}$$

where ${}_1F_1(a;b;z)$ is the the confluent hypergeometric function given in [60, eq. (9.210.1)].

Now the joint moments can be written in single integral form as

$$\mathbb{E}[z_1^{n_1},\cdots,z_n^{n_L}] = \int_0^\infty \exp(-t)\prod_{k=1}^{L}\Gamma(1+\frac{n_k}{\beta})(2\Omega^2)^{\frac{n_k}{\beta}}\ {}_1F_1\left(-\frac{n_k}{\beta};1;-\frac{\lambda^2 t}{1-\lambda^2}\right) dt. \tag{4.41}$$

Then, the single integral representation for the EGC output SNR can be expressed as

$$m_n = \frac{(2n)!E_s^n(2\Omega^2)^{\frac{2n}{\beta}}}{(LN_0)^n}\sum_{\substack{n_1,\cdots,n_L=0\\ n_1+\cdots+n_L=2n}}\int_0^\infty \exp(-t)\prod_{k=1}^{L}\ {}_1F_1\left(-\frac{n_k}{\beta};1;-\frac{\lambda^2 t}{1-\lambda^2}\right) A(k)dt \tag{4.42}$$

where $A(k) = \dfrac{\Gamma(1+\frac{n_k}{\beta})}{n_k!}$. The integral part of (4.42) can be identified as the Laplace transform of the product of L confluent hypergeometric functions where the Laplace transform variable s has the specific value of 1. Using the result [57, eq. (3.35.7.4)], the solution for the integral can be found in terms of the Lth-order Appell hypergeometric function [60, eq (9.19)], namely

$$\int_0^\infty \exp(-t) \prod_{k=1}^{L} {}_1F_1\left(-\frac{n_k}{\beta}; 1; -\frac{\lambda^2 t}{1-\lambda^2}\right) = F_A\left(1; -\frac{n_1}{\beta}, \cdots, -\frac{n_L}{\beta}; 1, \cdots, 1; x_1, \cdots, x_L\right) \quad (4.43)$$

where $x_i = -\dfrac{\lambda^2}{1-\lambda^2}$ for $i \in \{1, \cdots, L\}$. The region of convergence of the Appell hypergeometric function in (4.43) is constrained by $|x_1| + |x_2| + \cdots + |x_L| < 1$, [61, eq. xxxvii.$1^0$]. Therefore the convergence is limited to values of λ^2 ranging from $\dfrac{-1}{L-1}$ to $\dfrac{1}{L+1}$, and does not cover the full range of λ^2. However a transformation operation on the Appell hypergeometric function can be used to obtain a converging series for the hypergeometric function. Similar to [58], we use the transformation given in [61, eq. xxxviii 9_{2n}] and obtain

$$F_A\left(1; -\frac{n_1}{\beta}, \cdots, -\frac{n_L}{\beta}; 1, \cdots, 1; x_1, \cdots, x_L\right) = \frac{1-\lambda^2}{1+\lambda^2(L-1)} F_A\left(1; \theta_1, \cdots, \theta_L; 1, \cdots, 1; y_1, \cdots, y_L\right) \quad (4.44a)$$

$$\theta_i = 1 + -\frac{n_i}{\beta}, \qquad i \in \{1, \cdots, L\} \quad (4.44b)$$

$$y_i = \frac{\lambda^2}{1+\lambda^2(L-1)}, \qquad i \in \{1, \cdots, L\}. \quad (4.44c)$$

Since $|y_1| + |y_2| + \cdots + |y_L| = \dfrac{L\lambda^2}{L\lambda^2 + (1-\lambda^2)} < 1$, the Appell hypergeometric function in (4.44a) converges for the entire range of λ^2 such that $0 < \lambda^2 < 1$. Therefore the output SNR moments of EGC operating in equally correlated Weibull fading can be evaluated using

$$m_n = \frac{(2n)! E_s^n (2\Omega^2)^{\frac{2n}{\beta}}}{(LN_0)^n} \times \sum_{\substack{n_1, \cdots, n_L = 0 \\ n_1 + \cdots + n_L = 2n}} \frac{1-\lambda^2}{1+\lambda^2(L-1)} F_A\left(1; \theta_1, \cdots, \theta_L; 1, \cdots, 1; y_1, \cdots, y_L\right) \prod_{k=1}^{L} A(k). \quad (4.45)$$

In the following discussion, we consider some special cases of (4.45).

4.5.1 Average output SNR of the EGC

With the aid of [57, eq. (3.35.7.1)] and the relationship between the second order Appell hypergeometric function and the Gauss hypergeometric function given in [62, eq. (C.4)], the average output SNR for the EGC can be simplified as

$$\bar{\gamma}_{\text{egc}} = \frac{\bar{\gamma}}{\Gamma\left(\frac{2}{\beta}+1\right)}\Bigg[(1-\lambda^2)^{\frac{2}{\beta}+1}\Gamma\left(\frac{2}{\beta}+1\right)\ {}_2F_1\left(1+\frac{2}{\beta},1;1;\lambda^2\right) + (L-1)\left(\Gamma\left(\frac{1}{\beta}+1\right)\right)^2\ {}_2F_1\left(-\frac{1}{\beta},-\frac{1}{\beta};1;\lambda^4\right)\Bigg]. \tag{4.46}$$

For the special case of Rayleigh fading where $\beta = 2$, it can be shown that (4.46) simplifies to the previously known result in [58, eq. (19)], namely

$$\bar{\gamma}_{\text{egc}} = \bar{\gamma}\left[1+\frac{(L-1)\pi}{4}\ {}_2F_1\left(-\frac{1}{2},-\frac{1}{2};1;\lambda^4\right)\right]. \tag{4.47}$$

For uncorrelated branches where $\lambda = 0$, the average output SNR simplifies to

$$\bar{\gamma}_{\text{uncorrelated}} = \bar{\gamma}\left[1+(L-1)\frac{\left(\Gamma\left(\frac{1}{\beta}+1\right)\right)^2}{\Gamma\left(\frac{2}{\beta}+1\right)}\right]. \tag{4.48}$$

4.5.2 Second moment of EGC output SNR

The second moment of the EGC output SNR can be obtained as

$$\begin{aligned} m_2 = \frac{4!\bar{\gamma}^2}{L^2}\Bigg[&\binom{L}{1}\frac{\Gamma\left(1+\frac{4}{\beta}\right)(1-\lambda^2)^{1+\frac{4}{\beta}}}{4!\Gamma^2\left(1+\frac{2}{\beta}\right)}\ {}_2F_1\left(1+\frac{4}{\beta},1;1;\lambda^2\right) \\ &+\binom{L}{1}\ {}_2F_1\left(-\frac{2}{\beta},-\frac{2}{\beta};1;\lambda^4\right) \\ &+2\binom{L}{2}\frac{\Gamma\left(1+\frac{3}{\beta}\right)\Gamma\left(1+\frac{1}{\beta}\right)}{3!\Gamma^2\left(1+\frac{2}{\beta}\right)}\ {}_2F_1\left(1+\frac{4}{\beta},1;1;\lambda^2\right) \\ &+3\binom{L}{3}\frac{\Gamma^2\left(1+\frac{1}{\beta}\right)(1-\lambda^2)^{1+\frac{4}{\beta}}}{2\Gamma\left(1+\frac{2}{\beta}\right)(1+2\lambda^2)}F_A\left(1;1+\frac{1}{\beta},1+\frac{1}{\beta},1+\frac{2}{\beta};1,1,1;\theta_1,\theta_2,\theta_3\right) \\ &+\binom{L}{4}\frac{\Gamma^4\left(1+\frac{1}{\beta}\right)(1-\lambda^2)^{1+\frac{4}{\beta}}}{\Gamma^2\left(1+\frac{2}{\beta}\right)(1+3\lambda^2)}F_A\left(1;1+\frac{1}{\beta},\cdots,1+\frac{1}{\beta};1,1,1,1;\alpha_1,\alpha_2,\alpha_3,\alpha_4\right)\Bigg] \end{aligned} \tag{4.49a}$$

$$\theta_k = \lambda^2/(1+2\lambda^2), \qquad k \in \{1,2,3\} \tag{4.49b}$$

$$\alpha_k = \lambda^2/(1+3\lambda^2), \qquad k \in \{1,2,3,4\}. \tag{4.49c}$$

For the special case of dual branch diversity, (4.49a) simplifies to

$$m_2 = 3!\bar{\gamma}^2\left[\frac{1}{4}\,{}_2F_1\left(-\frac{2}{\beta},-\frac{2}{\beta};1;\lambda^4\right) + \frac{\Gamma\left(1+\frac{3}{\beta}\right)\Gamma\left(1+\frac{1}{\beta}\right)}{3\Gamma^2\left(1+\frac{2}{\beta}\right)}\,{}_2F_1\left(-\frac{3}{\beta},-\frac{1}{\beta};1;\lambda^4\right) + \frac{\Gamma\left(1+\frac{3}{\beta}\right)(1-\lambda^2)^{1+\frac{4}{\beta}}}{12\Gamma^2\left(1+\frac{2}{\beta}\right)}\,{}_2F_1\left(1+\frac{4}{\beta},1;1;\lambda^2\right)\right]. \tag{4.50}$$

4.5.3 Other moment based performance measures for EGC

Reference [58] presented an approach to compute the EGC output SNR CDF using the output SNR moments. Further in [58], moments of the EGC output SNR were used to evaluate the approximate average SER of EGC. The same approaches can be used for the case of equally correlated Weibull fading channels.

Also, the output SNR moments can be used to compute other moment based performance measures for the EGC such as central moments, kurtosis and amount of fading (AF), using the standard methodologies.

4.6 Numerical Results and Discussion

In this section, we present some example results obtained by numerically evaluating the expressions presented in Section 4.4.3. For simplicity, we consider the case when branch fadings are equally correlated and identically distributed. Also it is assumed that the symbols have unit power, i.e $E_s = 1$ and the additive Gaussian noise in all the branches have variance of unity, i.e. ($N_0 = 1$) in numerical evaluations and simulation results. Fig. 4.1 shows the outage probability of the system for different values of β, when the power correlation coefficient $\rho = \varrho^2$ of the underlying Rayleigh RVs is equal to 0.4. We observe the performance improvement with increasing β values and diversity order L. Fig. 4.2 shows the outage probability for different values of ρ and diversity order L, when $\beta = 2.5$. The performance loss due to branch correlation and the possible gains using additional antennas can be quantified from the figures. For example, when $\beta = 2.5$ and $\rho = 0.4$, a normalized SNR gain of 1.6 dB can be obtained by increasing the number of receiver antennas to 5

from 4, while the gain is 1.1 dB for an increase from 5 to 6. The normalized threshold γ^* is calculated as $\gamma_{th}/\bar{\gamma}$. Fig. 4.3 shows the average BER of BPSK signaling for the selection combiner operating in equally correlated Weibull fading at $\beta = 2.5$. We observe that the marginal SNR gain of an additional receiver antenna diminishes as the branch correlation increases, as expected. Fig. 4.4 shows the normalized average output SNR for a 4-branch selection combiner. We observe the negative impact of branch correlation on the output SNR. However, the average output SNR degrades with increasing fading parameter β, which is similar to the results observed for uncorrelated branch SC in Weibull fading channels [63].

Fig. 4.5 shows the effect of branch correlation on normalized average output SNR $\bar{\gamma}_{\text{egc}}/\bar{\gamma}$ for EGC in equally correlated Weibull fading. The average SNR increases as the branch correlation increases, which is opposite behaviour to the behaviour we observed for the SC case. An explanation for this phenomena was given in [56]. Also, it is interesting to note that the average SNR for EGC improves with the fading severity parameter β, while we observed the opposite for the selection combiner. Fig. 4.6 shows the effects of branch correlation and fading severity on the amount of fading for EGC. The AF improves with increasing fading parameter and decreasing branch correlation.

4.7 Summary

New single integral representations for the PDF and CDF of the multivariate Weibull distribution with constant correlation were derived. The new results were expressed using mathematical functions available in common mathematical software such as MATLAB. The new representation for the multivariate CDF was used to evaluate performance measures for a selection combining diversity receiver operating in equally correlated Weibull fading. New results for performance measures such as average SER, outage probability and average SNR were evaluated using single or double integrals for an arbitrary diversity order. Furthermore, the new multivariate PDF expression was used to evaluate the output SNR moments of an EGC operating in equally correlated Weibull fading channels. The output moments were expressed using single integrals or infinite series solutions. Numerical results for the performance indicators were obtained and simulation results were used to verify the accuracy of the theoretical analysis.

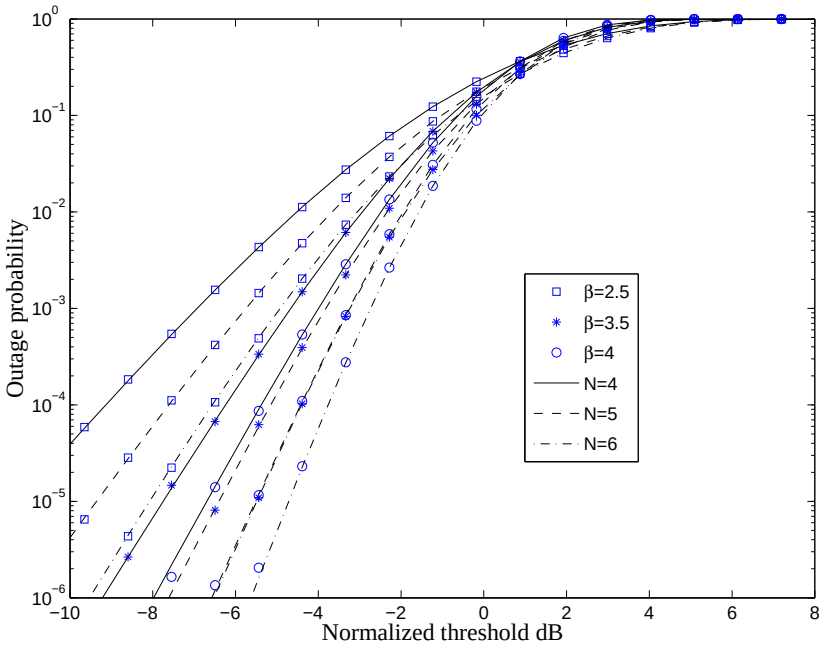

Figure 4.1. The effect of β on the outage probability of the selection combiner for the case when $\rho = 0.4$. The markers on the lines denote simulation results.

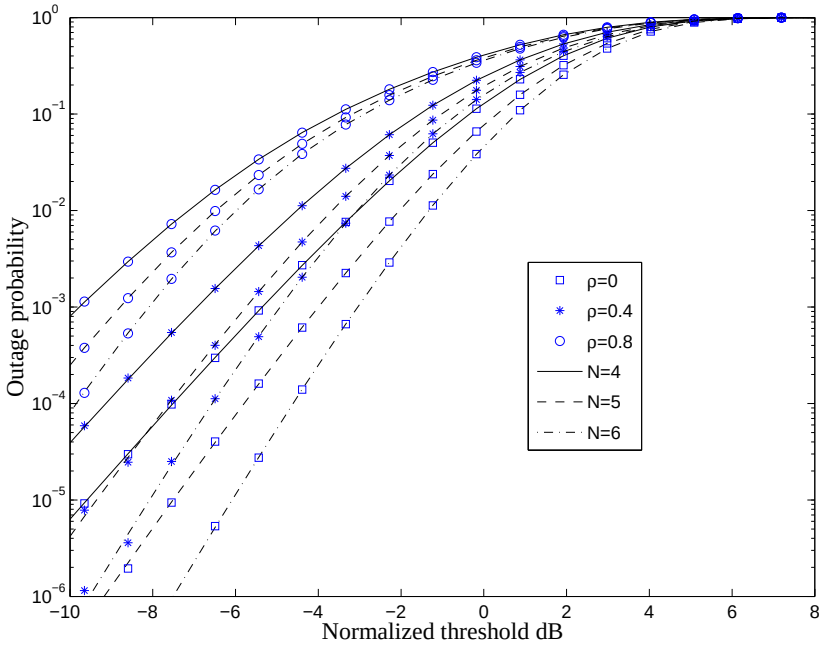

Figure 4.2. The effect of power correlation ρ on the outage probability of the selection combiner for the case when $\beta = 2.5$. The markers on the lines denote simulation results.

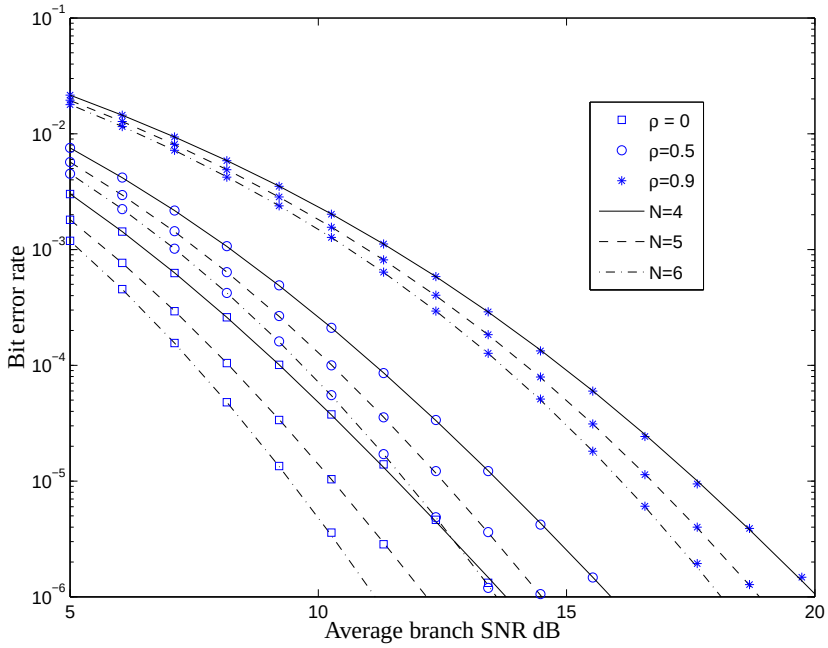

Figure 4.3. The effect of power correlation ρ on the average BER of BPSK in equally correlated Weibull fading.

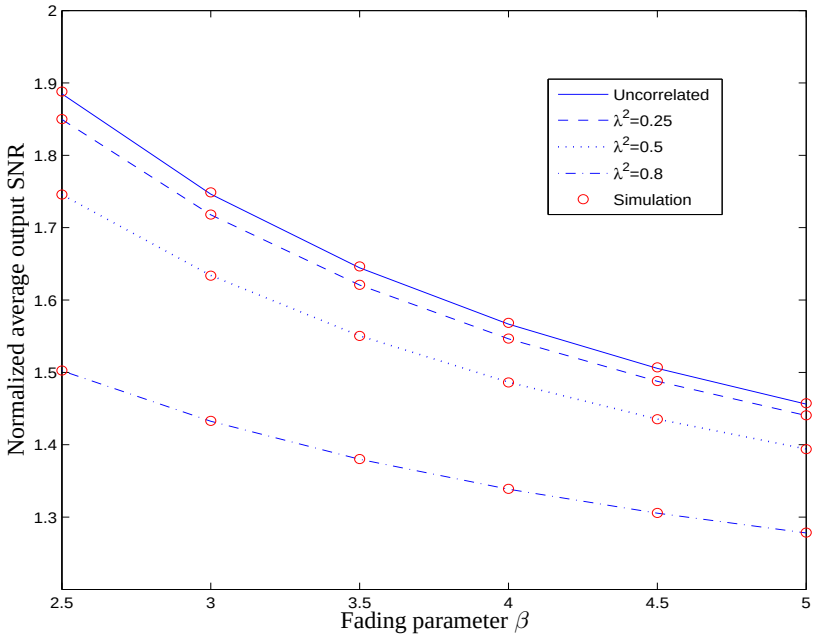

Figure 4.4. The average output SNR for a 4-branch selection combiner operating in equally correlated Weibull fading.

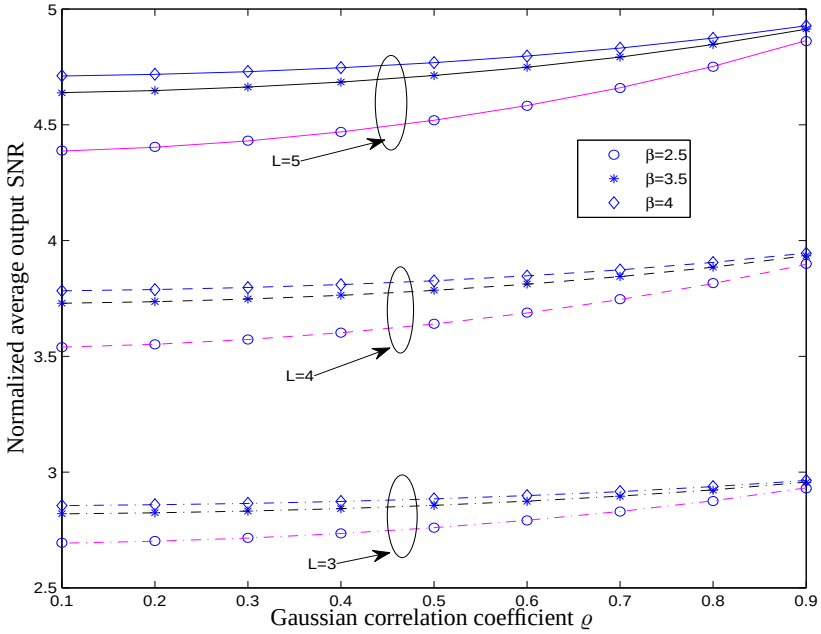

Figure 4.5. The average output SNR of EGC operating in equally correlated Weibull fading.

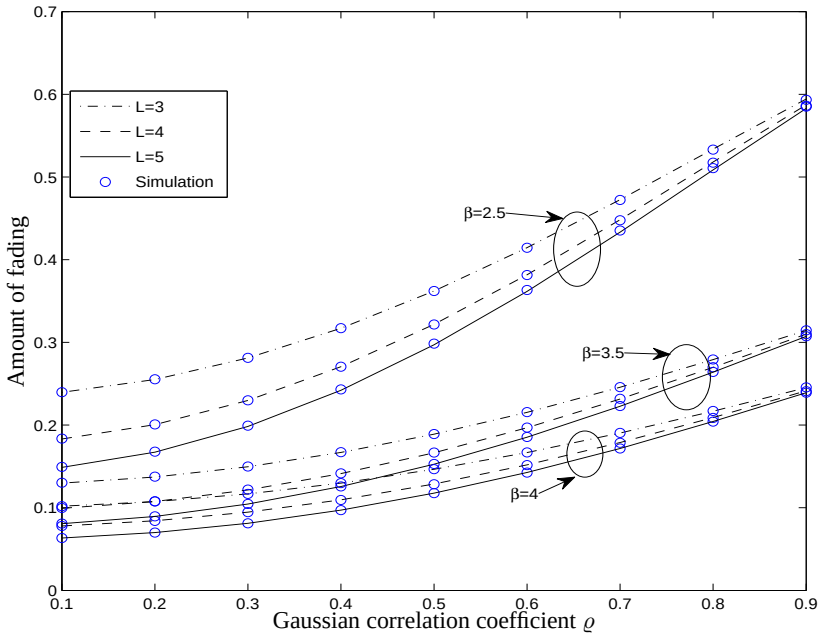

Figure 4.6. Reduction of the amount of fading using diversity for EGC operating in equally correlated Weibull fading.

Chapter 5

Simple SER Expressions for Dual Branch MRC in Correlated Nakagami-*q* Fading

5.1 Introduction

The Hoyt distribution [2] (also known as Nakagami-*q* [1]) is used to model wireless channels where the in-phase and quadrature signal components have zero means and arbitrary variances. Some results on performance evaluation of wireless communication systems with diversity reception, operating in independent Hoyt fading channels are found in [64], [65]. However, only a limited number of performance results are available for diversity in correlated Hoyt fading channels.

In reference [66], the outage probability of a dual MRC system operating in correlated Hoyt fading was studied for the general case of non-identically distributed branches. The results are given as a double integral of an infinite summation. The authors of [67] derived an infinite series solution for the average BER of binary coherent and noncoherent modulations with dual MRC in correlated Hoyt fading for the case of identically distributed branches. An infinite series solution for the outage probability of the system was also given in [67].

In this chapter[1], we present simple expressions for the SER of dual MRC in identically distributed correlated Hoyt fading channels. We use a decorrelation transformation, which was used on correlated branches in [69] for Rayleigh and Rician fading channels, to make the transformed branches independent of each other. Then we can easily compute the SER of coherent and noncoherent modulations using the decorrelated branches.

[1] A version of this chapter has been accepted for publication in the *IEEE Communications Letters* [68].

Other performance parameters such as the outage probability can also be evaluated using methodologies developed for independent fading branches.

The remainder of this chapter is organized as follows. In Section 5.2, we present the correlated Hoyt fading channel model and the decorrelation transformation on the correlated fading branches. New simple representations for average SER are given Section 5.3. Section 5.4 presents some numerical and simulation results.

5.2 Channel Model and Decorrelation Transformation

Let r_1 and r_2 denote the complex baseband equivalent signal samples at the two branches. We write

$$r_1 = g_1 x + n_1 \tag{5.1}$$

$$r_2 = g_2 x + n_2 \tag{5.2}$$

where x is the data symbol with energy E, $g_i, i = 1, 2$ are zero-mean complex Gaussian channel gains and $n_i, i = 1, 2$ are zero-mean Gaussian noise samples with variance N_0. The branch fadings are assumed to be identically distributed with average SNR, $\bar{\gamma}$.

Assuming slow, flat fading channels, we model the channel gains using the technique given in [41, eq. (8.1.6)] as

$$g_k = (\sqrt{1-\lambda^2} X_k + \lambda X_0) + j(\sqrt{1-\lambda^2} Y_k + \lambda Y_0), \quad k = 1, 2 \tag{5.3}$$

where $j = \sqrt{-1}$, $\lambda \in (-1, 1)$, $X_k (k = 0, 1, 2)$ are independent zero-mean Gaussian RVs with variance $\sigma_x^2/2$ and $Y_k (k = 0, 1, 2)$ are independent zero-mean Gaussian RVs with variance $\sigma_y^2/2$. Then g_k is a zero-mean complex Gaussian RV with real and imaginary parts having unequal variances for $\sigma_x \neq \sigma_y$. Therefore $|g_k|$ is Hoyt distributed with mean-square value $\mathbb{E}[|g_k|^2] = \frac{\sigma_x^2 + \sigma_y^2}{2}$ and Hoyt parameter $q = \frac{\sigma_x}{\sigma_y}$, $0 < q \leq 1$. It can be shown that the correlation coefficient between g_1, g_2 is given by

$$\rho = \frac{\mathbb{E}[g_1 g_2^*] - \mathbb{E}[g_1]\mathbb{E}[g_2^*]}{\sqrt{\mathbb{E}[|g_1|^2]\mathbb{E}[|g_2|^2]}} = \lambda^2. \tag{5.4}$$

The power correlation of the two fading gains can be computed using [70, eq. (11)].

Now we apply the decorrelation transformation used in [69] on r_1 and r_2 and obtain the transformed branches as

$$w_1 = \frac{r_1 + r_2}{\sqrt{2}} = \frac{g_1 + g_2}{\sqrt{2}} x + \frac{n_1 + n_2}{\sqrt{2}} = G_1 x + v_1 \tag{5.5}$$

and

$$w_2 = \frac{r_1 - r_2}{\sqrt{2}} = \frac{g_1 - g_2}{\sqrt{2}}x + \frac{n_1 - n_2}{\sqrt{2}} = G_2 x + v_2. \tag{5.6}$$

It can be easily shown that G_1 and G_2 are uncorrelated, and since they are complex jointly Gaussian RVs, they are independent. Similarly we can show that the additive noise terms v_1 and v_2 are independent Gaussian RVs with variance N_0. Also we note that $|G_1|$ and $|G_2|$ are Hoyt distributed with Hoyt parameter q and mean-square values $\frac{(1+\lambda^2)(\sigma_x^2+\sigma_y^2)}{2}$ and $\frac{(1-\lambda^2)(\sigma_x^2+\sigma_y^2)}{2}$, respectively.

The output of the dual MRC receiver is computed as

$$y_c = g_1^* \times r_1 + g_2^* \times r_2. \tag{5.7}$$

Then the decision statistic is given by

$$z_o = (|g_1|^2 + |g_2|^2)x + g_1^* n_1 + g_2^* n_2. \tag{5.8}$$

We can easily show that an identical decision statistic can be achieved with the transformed branches by computing

$$y_d = G_1^* \times w_1 + G_2^* \times w_2. \tag{5.9}$$

Therefore, the decorrelation does not alter the performance of the MRC receiver operating in Hoyt channels. In [71], a similar result was proved for Rayleigh and Rician channels.

5.3 Simple Expressions for Average SER

Let γ_1 and γ_2 denote the instantaneous SNRs of w_1 and w_2, respectively. The average SNRs $\bar{\gamma_1}$ and $\bar{\gamma_2}$ are

$$\bar{\gamma_1} = \frac{\mathbb{E}[|G_1|^2]E}{N_0} = (1+\lambda^2)\bar{\gamma} \tag{5.10}$$

$$\bar{\gamma_2} = \frac{\mathbb{E}[|G_2|^2]E}{N_0} = (1-\lambda^2)\bar{\gamma}. \tag{5.11}$$

Then the MGF $M_{\gamma_i}(s)$ of $\gamma_i, i = 1, 2$ can be written as [3]

$$M_{\gamma_i}(s) = \left(1 - 2s\bar{\gamma_i} + \frac{(2s\bar{\gamma_i})^2 q^2}{(1+q^2)^2}\right)^{-\frac{1}{2}}. \tag{5.12}$$

Since the SNRs of the decorrelated branches are independent, we obtain the MGF of the output SNR for dual MRC in correlated Hoyt fading as

$$M_{\gamma_{\mathrm{MRC}}}(s) = M_{\gamma_1}(s).M_{\gamma_2}(s) \tag{5.13a}$$

and

$$M_{\gamma_{\mathrm{MRC}}}(s) = \left(1 - 2s\bar{\gamma_1} + \frac{(2s\bar{\gamma_1})^2 q^2}{(1+q^2)^2}\right)^{-\frac{1}{2}} \left(1 - 2s\bar{\gamma_2} + \frac{(2s\bar{\gamma_2})^2 q^2}{(1+q^2)^2}\right)^{-\frac{1}{2}}. \quad (5.13b)$$

Now we can easily compute some performance measures for dual MRC using standard procedures available for independent non-identically distributed fading channels [3]. The well known MGF based approach can be used to obtain simple expressions for average SER of dual MRC in identically distributed correlated Hoyt fading for a large family of coherent and noncoherent modulation schemes.

SER of M-AM

The average SER for M-ary amplitude modulation (M-AM) signals can be computed using

$$\bar{P_s} = \frac{2(M-1)}{M\pi} \int_0^{\pi/2} M_{\gamma_{\mathrm{MRC}}}\left(-\frac{g_{AM}}{sin^2(\phi)}\right) d\phi \quad (5.14)$$

where $g_{AM} = 3/(M^2-1)$.

SER of M-PSK

The average SER for M-ary phase shift keying (M-PSK) signals can be evaluated using

$$\bar{P_s} = \frac{1}{\pi} \int_0^{\frac{(M-1)\pi}{M}} M_{\gamma_{\mathrm{MRC}}}\left(-\frac{g_{PSK}}{sin^2(\phi)}\right) d\phi \quad (5.15)$$

where g_{PSK} is given by $sin^2(\pi/M)$.

SER of M-QAM

The average SER for square M-ary quadrature amplitude modulation (M-QAM) signals can be calculated using

$$\bar{P_s} = \frac{4}{\pi}\left(1 - \frac{1}{\sqrt{M}}\right) \int_0^{\pi/2} M_{\gamma_{\mathrm{MRC}}}\left(-\frac{g_{QAM}}{sin^2(\phi)}\right) d\phi - \frac{4}{\pi}\left(1 - \frac{1}{\sqrt{M}}\right)^2 \int_0^{\pi/4} M_{\gamma_{\mathrm{MRC}}}\left(-\frac{g_{QAM}}{sin^2(\phi)}\right) d\phi \quad (5.16)$$

where g_{QAM} is equal to $3/(2(M-1))$.

SER of M-FSK

The MGF approach can be used to evaluate the average SER of M-ary frequency shift keying (MFSK) as

$$\bar{P}_s = \sum_{n=1}^{M-1} \frac{(-1)^{n+1}\binom{M-1}{n}}{n+1} M_{\gamma_{\mathrm{MRC}}}\left(\frac{n}{n+1}\right). \tag{5.17}$$

BER of noncoherent BFSK

The average BER of noncoherent binary frequency shift keying (BFSK) and differential BPSK can be calculated according to

$$\bar{P}_b = a M_{\gamma_{\mathrm{MRC}}}(b) \tag{5.18}$$

where $(a, b) = (0.5, 0.5)$ for noncoherent BFSK and $(a, b) = (0.5, 1)$ for differential BPSK.

It is important to note that the new expressions for SER are given as finite range single integrals of elementary mathematical functions. All the expressions can be easily evaluated numerically using mathematical software packages such as MATLAB and MATHEMATICA. The time required to compute the new solutions is significantly lower than the time required to compute the infinite summation solutions given in [67]. Also note that the use of the decorrelation transformation enables the use of efficient numerical techniques [3, eq. 9.186] to compute the outage probability of the dual MRC receiver in correlated Hoyt fading.

5.4 Numerical Results and Discussion

In this section, we present some example results obtained by numerically evaluating the SER expressions presented in Section 5.3. Fig. 5.1 shows the average BER for coherent BPSK with dual MRC in correlated Hoyt fading for different values of ρ and q. We can clearly quantify the performance degradation with increasing correlation coefficient and decreasing q values. Fig. 5.2 shows the average SER for 8-PSK signaling in correlated Hoyt fading. We observe an SNR loss of 1.5 dB when ρ changes from 0 to 0.7 with $q = 0.5$ and the loss is 1 dB when $q = 0.1$. Also, the SNR losses for the case when ρ changes from 0.7 to 0.9 can be quantified as 2 dB for $q = 0.5$ and 1.5 dB for $q = 0.1$. Fig. 5.3

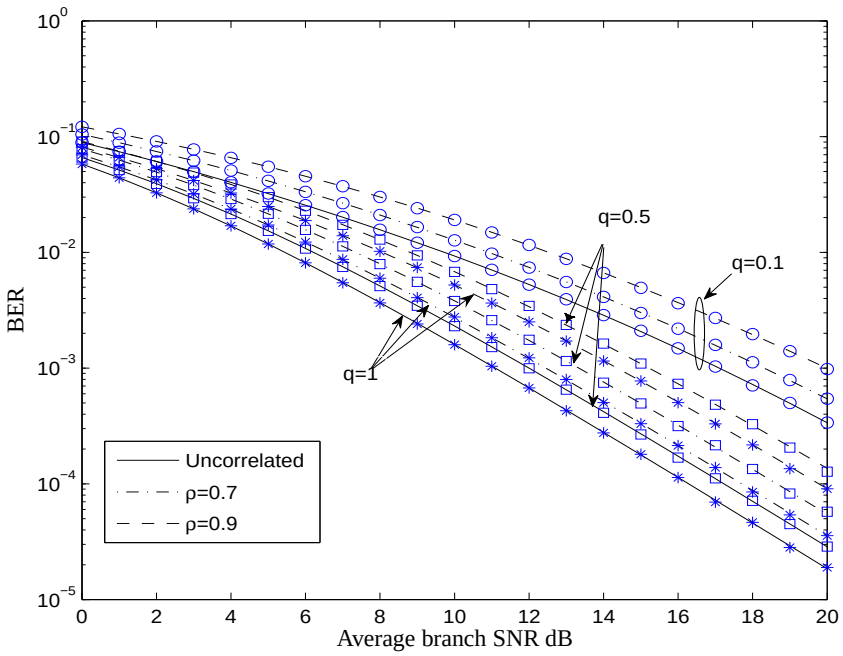

Figure 5.1. The average BER of coherent BPSK with Hoyt parameter q and correlation coefficient ρ.

shows the average SER for 16-QAM signaling with dual MRC in correlated Hoyt fading. The SNR losses observed in 16-QAM show similar behavior to those observed in 8-PSK. In the figures, lines are used to denote the numerical values obtained from the theory. The markers denote the corresponding SER result obtained from Monte-Carlo simulation, where the MRC receiver does not employ decorrelation before decoding. We note the excellent agreement of numerical results and simulation results in all the cases. This confirms that the decorrelation does not alter the MRC performance and that the new SER results are accurate.

5.5 Summary

It was shown that using a decorrelation transformation on the correlated branches, we can obtain simple expressions for the average SER of several coherent and noncoherent signaling formats with dual MRC in identically distributed correlated Hoyt fading. The expressions were obtained as finite range single integrals of basic mathematical functions, which can be easily and rapidly evaluated with common mathematical software. Simulation results were given to verify the accuracy of the analytical solutions proposed in this chapter.

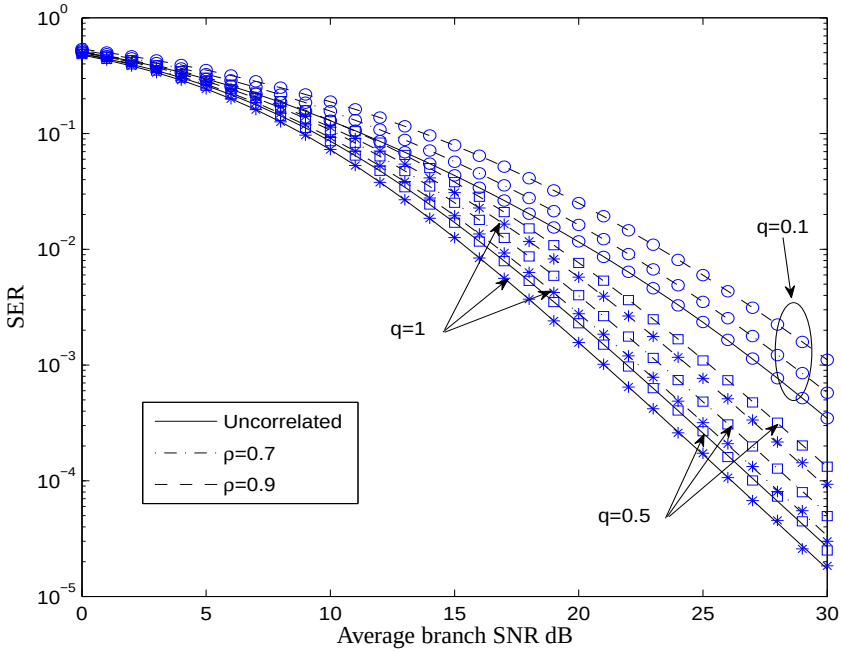

Figure 5.2. The average SER of 8-PSK with different values of Hoyt parameter q and correlation coefficient ρ.

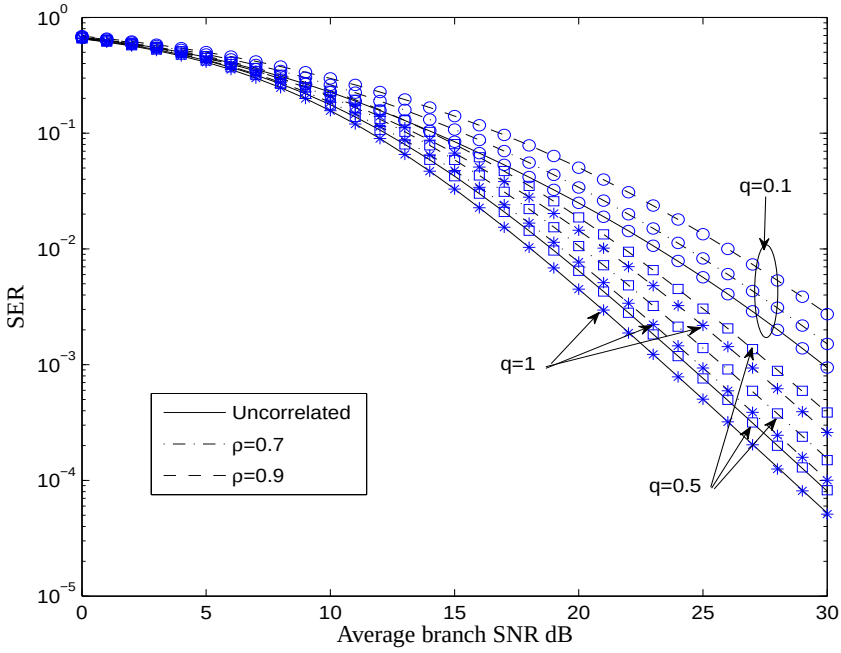

Figure 5.3. The average SER of 16-QAM with different values of Hoyt parameter q and correlation coefficient ρ.

Chapter 6

Conclusions and Future Research Directions

In this chapter, we conclude this thesis while providing some insights into future research directions based on the results of this thesis.

6.1 Conclusions

This thesis presented a framework to derive new mathematical representations for the multivariate PDF and CDF of some popular statistical distributions used in wireless communication theory. The constant correlation model and a generalized correlation structure was used in our analysis.

- Chapter 2 presented new representations for multivariate PDF and CDF of Rayleigh, Rician and Nakagami-*m* distributions with a generalized correlation structure. The new representations were given as single integral solutions, which can be readily evaluated with common mathematical software such as MATLAB. The new representations were used to evaluate the performance of selection diversity combiners operating in correlated Rayleigh, Rician and Nakagami-*m* fading channels.

- New representations for the multivariate non-central χ^2 distribution with constant correlation were presented in Chapter 3. The new multivariate PDF and CDF expressions were given as single integral solutions, which can be easily and rapidly evaluated with MATLAB. The new distribution representations were shown to be useful in analyzing MIMO systems operating in correlated Rician fading channels.

- Chapter 4 presented new multivariate PDF and CDF expressions for the Weibull distribution with constant correlation. Similar to the results of Chapters 2 and 3, the new

multivariate Weibull PDF and CDF were given as single integral solutions, which can be easily evaluated with MATLAB. The new Weibull CDF expression was used to analyze the performance of a selection diversity combiner operating in correlated Weibull fading channels, while the new PDF expression was used to analyze the output SNR moments of EGC operating in correlated Weibull fading channels.

- In Chapter 5, we presented a new technique to analyze performance of a dual MRC receiver operating in identically distributed Nakagami-*q* fading channels. It was shown that by using a decorrelation transformation on the correlated diversity branches, they can be made independent. Then we used the standard performance analysis methodologies available for independent fading channels to obtain new simple and rapidly computable expressions for performance measures of the dual-branch MRC receiver operating in Hoyt fading.

6.2 Future Research Directions

The following may be considered as possible future research directions based on this thesis.

- This foundation may be used as a starting point to derive new multivariate PDF and CDF representations for several other interesting distributions such as the log-normal distribution, $\kappa - \mu$ distribution and other general fading distributions.

- One can consider about methodologies which can be used to widen the number of classes of correlation matrices which can be included in the framework presented in Chapter 2.

- The framework presented in this thesis may be useful for study of relay networks with nodes consisting of multiple antennas.

- Another possible research direction will be to consider the applicability of the framework proposed in this thesis for wireless communication systems with imperfect channel state information.

- Furthermore, one can apply the multivariate distribution expressions introduced in this thesis to several other areas other than wireless communication system performance analysis. For an example, the Weibull distribution is used in other interesting applications such as weather forecasting, reliability engineering and failure data analysis. The new representations of multivariate Weibull PDF and CDF may useful in

the above mentioned areas. Also the non-central chi-square distribution is widely used in other areas of statistics such as hypothesis testing. Therefore the derived new representations may be used to develop new results.

Bibliography

[1] M. Nakagami, "The *m*-distribution, a general formula of intensity distribution of rapid fading," *Statistical Methods in Radio Wave Propagation*, 1960.

[2] R. S. Hoyt, "Probability functions for the modulus and angle of the normal complex variate," *Bell Systems Tech. J.*, vol. 26, pp. 318–359, 1947.

[3] M. K. Simon and M. S. Alouini, *Digital communication over fading channels*. Hoboken, New Jersey: John Wiley & sons, Inc., 2005.

[4] F. Babich and G. Lombardi, "Statistical analysis and characterization of the indoor propagation channel," *IEEE Trans. Commun.*, vol. 48, no. 3, pp. 455–464, Mar. 2000.

[5] N. S. Adawi *et al.*, "Coverage prediction for mobile radio systems operating in the 800/900 MHz frequency range," *IEEE Trans. Veh. Technol.*, vol. 37, pp. 3–72, Feb. 1988.

[6] N. C. Sagias and G. K. Karagiannidis, "Gaussian class multivariate Weibull distributions: theory and applications in fading channels," *IEEE Trans. Inf. Theory*, vol. 51, no. 10, pp. 3608–3619, Oct. 2005.

[7] M. D. Yacoub, "The $\kappa - \mu$ distribution and the $\eta - \mu$ distribution," *IEEE Antennas Propag. Mag.*, vol. 49, no. 1, pp. 68–81, Feb. 2007.

[8] ——, "The α-μ distribution: A physical fading model for the Stacy distribution," *IEEE Trans. Veh. Technol.*, vol. 56, no. 1, pp. 27–34, 2007.

[9] A. Abdi, H. A. Barger, and M. Kaveh, "A simple alternative to the lognormal model of shadow fading in terrestrial and satellite channels," in *IEEE 54th Vehicular Technology Conference, VTC 2001 Fall.*, vol. 4, Atlantic City, NJ, Jan. 2001, pp. 2058–2062.

[10] V. A. Aalo, "Performance of maximal-ratio diversity systems in a correlated Nakagami-fading environment," *IEEE Trans. Commun.*, vol. 43, no. 8, pp. 2360–2369, Aug. 1995.

[11] R. D. Vaughan and B. Anderson, "Antenna diversity in mobile communications," *IEEE Trans. Veh. Technol.*, vol. 36, no. 4, pp. 149–172, 1987.

[12] Y. Chen and C. Tellambura, "Distribution functions of selection combiner output in equally correlated Rayleigh, Rician, and Nakagami-*m* fading channels," *IEEE Trans. Commun.*, vol. 52, no. 11, pp. 1948–1956, Nov. 2004.

[13] K. S. Miller, *Multidimensional Gaussian Distributions*. New York: Wiley, 1964.

[14] R. K. Mallik, "On multivariate Rayleigh and exponential distributions," *IEEE Trans. Inform. Theory.*, vol. 49, no. 6, pp. 1499–1515, Jun. 2003.

[15] C. C. Tan and N. C. Beaulieu, "Infinite series representations of the bivariate Rayleigh and Nakagami-*m* distributions," *IEEE Trans. Commun.*, vol. 45, no. 10, pp. 1159–1161, Oct 1997.

[16] M. K. Simon and M.-S. Alouini, "A simple single integral representation of the bivariate Rayleigh distribution," *IEEE Commun. Lett.*, vol. 2, no. 5, pp. 128–130, May 1998.

[17] D. Middleton, *An Introduction to Statistical Communication Theory*. New York: McGraw-Hill, 1964.

[18] D. A. Zogas and G. K. Karagiannidis, "Infinite-series representations associated with the bivariate Rician distribution and their applications," *IEEE Trans. Commun.*, vol. 53, no. 11, pp. 1790–1794, Nov. 2005.

[19] M. K. Simon, "Comments on "Infinite-series representations associated with the bivariate Rician distribution and their applications"," *IEEE Trans. Commun.*, vol. 54, no. 8, pp. 1511–1512, Aug. 2006.

[20] P. Dharmawansa, N. Rajatheva, and C. Tellambura, "On the trivariate Rician distribution," *IEEE Trans. Commun.*, vol. 56, no. 12, pp. 1993–1997, Dec. 2008.

[21] A. A. Abu-Dayya and N. C. Beaulieu, "Switched diversity on microcellular Ricean channels," *IEEE Trans. Veh. Technol.*, vol. 43, no. 4, pp. 970–976, Nov. 1994.

[22] P. Bello and C. Boardman, "Effect of multipath on ranging error for an airplane-satellite link," *IEEE Trans. Commun.*, vol. 21, no. 5, pp. 564–576, May 1973.

[23] J. Reig, L. Rubio, and N. Cardona, "Bivariate Nakagami-*m* distribution with arbitrary fading parameters," *Electronics Letters*, vol. 38, no. 25, pp. 1715–1717, Dec. 2002.

[24] G. K. Karagiannidis, D. A. Zogas, and S. A. Kotsopoulos, "On the multivariate Nakagami-*m* distribution with exponential correlation," *IEEE Trans. Commun.*, vol. 51, no. 8, pp. 1240–1244, Aug. 2003.

[25] P. Dharmawansa, N. Rajatheva, and C. Tellambura, "Infinite series representations of the trivariate and quadrivariate Nakagami-*m* distributions," *IEEE Trans. Wireless Commun.*, vol. 6, no. 12, pp. 4320–4328, Dec. 2007.

[26] R. A. A. de Souza and M. D. Yacoub, "Bivariate Nakagami-*m* distribution with arbitrary correlation and fading parameters," *IEEE Trans. Wireless Commun.*, vol. 7, pp. 5227–5232, Dec. 2008.

[27] K. Peppas and N. C. Sagias, "A trivariate Nakagami-*m* distribution with arbitrary covariance matrix and applications to generalized-selection diversity receivers," *IEEE Trans. Commun.*, vol. 57, no. 7, pp. 1896–1902, Jul. 2009.

[28] R. A. A. de Souza and M. D. Yacoub, "On the multivariate Nakagami-*m* distribution with arbitrary correlation and fading parameters," in *Proc. IEEE Int. Microwave and Optoelectronics Conf. (IMOC 2007).*, Oct./Nov. 2007, pp. 812–816.

[29] Y. Chen and C. Tellambura, "Infinite series representations of the trivariate and quadrivariate Rayleigh distribution and their applications," *IEEE Trans. Commun.*, vol. 53, no. 12, pp. 2092–2101, Dec. 2005.

[30] G. K. Karagiannidis, D. A. Zogas, and S. A. Kotsopoulos, "An efficient approach to multivariate Nakagami-*m* distribution using Green's matrix approximation," *IEEE Trans. Wireless Commun.*, vol. 2, no. 5, pp. 883–889, Sep. 2003.

[31] G. C. Alexandropoulos, N. C. Sagias, F. I. Lazarakis, and K. Berberidis, "New results for the multivariate Nakagami-*m* fading model with arbitrary correlation matrix and applications," *IEEE Trans. Wireless Commun.*, vol. 8, no. 1, pp. 245–255, Jan. 2009.

[32] T. Royen, "On some central and non-central multivariate chi-square distributions," *Statistica sinica.*, vol. 5, pp. 373–397, 1995.

[33] P. Dharmawansa, N. Rajatheva, and C. Tellambura, "New series representation for the trivariate non-central chi-squared distribution," *IEEE Trans. on Commun.*, vol. 57, no. 3, pp. 665–675, Mar. 2009.

[34] P. Dharmawansa and M. R. McKay, "Diagonal distribution of a complex non-central Wishart matrix: A new trivariate non-central chi-squared density," *J. Multivariate Anal.*, vol. 100, no. 4, pp. 561 – 580, Apr. 2009.

[35] G. C. Alexandropoulos, N. C. Sagias, and K. Berberidis, "On the multivariate Weibull fading model with arbitrary correlation matrix," *IEEE Antennas Wireless Propag. Lett.*, vol. 6, pp. 93–95, 2007.

[36] Z. G. Papadimitriou, P. T. Mathiopoulos, and N. C. Sagias, "The trivariate and quadrivariate Weibull fading distributions with arbitrary correlation and their applications to diversity reception," *IEEE Trans. Commun.*, vol. 57, no. 11, pp. 3230 –3234, Nov. 2009.

[37] R. A. A. de Souza and M. D. Yacoub, "The multivariate α- μ distribution," *IEEE Trans. Wireless Commun.*, vol. 9, no. 1, pp. 45 –50, Jan. 2010.

[38] K. T. Hemachandra and N. C. Beaulieu, "Novel simple forms for multivariate Nakagami-*m* distribution with generalized correlation," in *IEEE Wireless Communications and Networking Conference (IEEE WCNC 2010 - Physical)*, Sydney, Australia, Apr. 2010.

[39] N. C. Beaulieu and K. T. Hemachandra, "New simple solutions for the bivariate Rician PDF and CDF," in *IEEE Wireless Communications and Networking Conference*, Sydney, Australia, Apr. 2010.

[40] X. Zhang and N. C. Beaulieu, "Performance analysis of generalized selection combining in generalized correlated Nakagami-*m* fading," *IEEE Trans. Commun.*, vol. 54, no. 11, pp. 2103–2112, Nov. 2006.

[41] Y. Tong, *The Multivariate Normal Distribution*. New York: Springer-Verlag, 1990.

[42] W. C. Jakes, *Microwave Mobile Communications*. New York: IEEE press, 1994.

[43] J. G. Proakis and M. Salehi, *Digital Communications*, 5th ed. New York: McGraw Hill, 2008.

[44] A. Papoulis and U. S. Pillai, *Probability, Random Variables and Stochastic Processes*, 4th ed. New York: McGraw-Hill, 2002.

[45] S. O. Rice, "Mathematical analysis of random noise," *Bell Systems Tech. J.*, vol. 23, pp. 282–332, 1944.

[46] A. P. Prudnikov, Y. A. Brychkov, and O. I. Marichev, *Integrals and Series*. Gorden and Breach Science, 1990, vol. 4.

[47] G. L. Stüber, *Principles of Mobile Communication*. Norwell: Kluwer Academic, 2001.

[48] F. Haber and M. Noorchashm, "Negatively correlated branches in frequency diversity systems to overcome multipath fading," *IEEE Trans. Commun.*, vol. 22, no. 2, pp. 180–190, Feb. 1974.

[49] L. C. Andrews, *Special Functions of Mathematics for Engineers*, 2nd ed. Oxford : Oxford university press, 1998.

[50] A. F. Molisch and M. Z. Win, "MIMO systems with antenna selection," *IEEE Microw. Mag.*, vol. 5, no. 1, pp. 46–56, Mar. 2004.

[51] S. Sanayei and A. Nosratinia, "Antenna selection in MIMO systems," *IEEE Commun. Mag.*, vol. 42, no. 10, pp. 68–73, Oct. 2004.

[52] Z. Xu, S. Sfar, and R. S. Blum, "Analysis of MIMO systems with receive antenna selection in spatially correlated Rayleigh fading channels," *IEEE Trans. Veh. Technol.*, vol. 58, no. 1, pp. 251–262, Jan. 2009.

[53] H. Shen and A. Ghrayeb, "Analysis of the outage probability for spatially correlated MIMO channels with receive antenna selection," in *Global Telecommunications Conference, 2005. GLOBECOM '05. IEEE*, vol. 5, St. Louis, MO, Dec. 2005.

[54] R. K. Mallik and M. Z. Win, "Analysis of hybrid selection/maximal-ratio combining in correlated Nakagami fading," *IEEE Trans. Commun.*, vol. 50, no. 8, pp. 1372–1383, Aug 2002.

[55] K. T. Hemachandra and N. C. Beaulieu, "New representations for the multivariate Weibull distribution with constant correlation," *IEEE Global Communication Conference, Miami, FL, USA*, Dec. 2010, (Accepted).

[56] D. A. Zogas, N. C. Sagias, G. S. Tombras, and G. K. Karagiannidis, "Average output SNR of equal-gain diversity receivers over correlative Weibull fading channels," *European Trans. Teleommun.*, vol. 16, pp. 521–525, 2005.

[57] A. P. Prudnikov, Y. Brychkov, and O. Marichev, *Integrals and Series*. Gorden and Breach Science, 1998, vol. 4.

[58] Y. Chen and C. Tellambura, "Moment analysis of the equal gain combiner output in equally correlated fading channels," *IEEE Trans. Veh. Technol.*, vol. 54, no. 6, pp. 1971–1979, Nov. 2005.

[59] G. K. Karagiannidis, "Moments-based approach to the performance analysis of equal gain diversity in Nakagami-*m* fading," *IEEE Trans. Commun.*, vol. 52, pp. 685–690, Oct. 2000.

[60] I. Gradshteyn and I. Ryzhik, *Table of Integrals, Series, and Products, Seventh Edition*. Academic Press, 2007.

[61] P. Appell and J. K. de Fériet, *Hypergéométriques et hypersphériques - Polynomes d'Hermite*. Paris : Gauthier - Villars, 1926.

[62] A. Annamalai, C. Tellambura, and V. K. Bhargava, "Equal-gain diversity receiver performance in wireless channels," *IEEE Trans. Commun.*, vol. 48, pp. 1732–1745, Oct. 2000.

[63] N. C. Sagias, P. T. Mathiopoulos, and G. S. Tombras, "Selection diversity receivers in Weibull fading: outage probability and average signal-to-noise ratio," *Electronics Lett.*, vol. 39, pp. 1859–1860, Dec. 2003.

[64] M. K. Simon and M. Alouini, "A unified approach to the performance analysis of digital communication over generalized fading channels," *Proc. IEEE*, vol. 86, no. 9, pp. 1860–1877, Sep. 1998.

[65] A. Annamalai, C. Tellambura, and V. K. Bhargava, "Simple and accurate methods for outage analysis in cellular mobile radio systems-a unified approach," *IEEE Trans. Commun.*, vol. 49, no. 2, pp. 303–316, Feb. 2001.

[66] R. A. A. de Souza and M. D. Yacoub, "Maximal-ratio and equal-gain combining in Hoyt (Nakagami-*q*) fading," in *Veh. Technol. Conf., 2009. (VTC'09). IEEE 69th*, Barcelona, Apr. 2009, pp. 1–5.

[67] R. Subadar and P. R. Sahu, "Performance analysis of dual MRC receiver in correlated Hoyt fading channels," *IEEE Commun. Lett.*, vol. 13, no. 6, pp. 405–407, Jun. 2009.

[68] K. T. Hemachandra and N. C. Beaulieu, "Simple expressions for the SER of dual MRC in correlated Nakagami-*q* (Hoyt) fading," *IEEE Commun. Lett.*, (to appear).

[69] S. Haghani and N. C. Beaulieu, "On decorrelation in dual-branch diversity systems," *IEEE Trans. Commun.*, vol. 57, no. 7, pp. 2138–2147, Jul. 2009.

[70] J. R. Mendes, M. D. Yacoub, and G. Fraidenraich, "Closed-form generalized power correlation coefficient of the Hoyt fading signal," *IEEE Commun. Lett.*, vol. 10, no. 2, pp. 94–96, Feb. 2006.

[71] X. Dong and N. C. Beaulieu, "Optimal maximal ratio combining with correlated diversity branches," *IEEE Commun. Lett.*, vol. 6, no. 1, pp. 22–24, Jan. 2002.